



Universiteit
Leiden
The Netherlands

Disentangling a complex genus: systematics, biogeography and bioactivity of the genus *Phyllanthus* L. and related genera of tribe Phyllantheae (Phyllanthaceae)

Bouman, R.W.

Citation

Bouman, R. W. (2022, December 6). *Disentangling a complex genus: systematics, biogeography and bioactivity of the genus *Phyllanthus* L. and related genera of tribe Phyllantheae (Phyllanthaceae)*. Retrieved from <https://hdl.handle.net/1887/3492676>

Version: Publisher's Version

License: [Licence agreement concerning inclusion of doctoral thesis in the Institutional Repository of the University of Leiden](#)

Downloaded from: <https://hdl.handle.net/1887/3492676>

Note: To cite this publication please use the final published version (if applicable).

CHAPTER 9

Multiple continental dispersal events and radiation events underlie the modern-day diversity of tribe Phyllanthae (Phyllanthaceae)

Roderick W. Bouman, Paul J.A. Keßler, Ian R.H. Telford,
Jeremy J. Bruhl, Joeri S. Strijk, Richard M.K. Saunders,
Peter C. van Welzen

Submitted for publication in *Biological Journal of the Linnean Society*

Chapter 9

Multiple continental dispersal events and radiation events underlie the modern-day diversity of tribe Phyllanthae (Phyllanthaceae)

Short title: Historical biogeography of tribe Phyllanthae

Roderick W. Bouman^{1,2,3*}, Paul J.A. Keßler^{2,3}, Ian R.H. Telford⁴, Jeremy J. Bruhl⁴, Joeri S. Strijk^{5,6}, Richard M.K. Saunders⁷, Peter C. van Welzen^{1,3}

¹ Naturalis Biodiversity Center, PO Box 9517, 2300 RA Leiden, the Netherlands

² Hortus botanicus Leiden, Leiden University, PO Box 9500, 2300 RA Leiden, the Netherlands

³ Institute of Biology Leiden, Leiden University, PO Box 9505, 2300 RA Leiden, the Netherlands

⁴ Botany and N. C. W. Beadle Herbarium, School of Environmental and Rural Science, University of New England, Armidale, NSW 2351, Australia

⁵ Institute for Biodiversity and Environmental Research, Universiti Brunei Darussalam, Jalan Tungku Link, Brunei Darussalam

⁶ Alliance for Conservation Tree Genomics, Pha Tad Ke Botanical Garden, PO Box 959, 06000 Luang Prabang, Lao PDR

⁷ Division of Ecology & Biodiversity, School of Biological Sciences, The University of Hong Kong, Pokfulam Road, Hong Kong, China

Abstract

Several hypotheses have been invoked to explain the pantropical distribution of many plant taxa today. In this study, we reconstruct the historical biogeography of the monophyletic tribe Phyllanthae, of which the majority consists of *Phyllanthus* s.l. and study the processes that have given rise to the clade's pantropical distribution. A molecular dataset consisting of two nuclear markers and three plastid markers was analysed in BEAST to reconstruct divergence times for 212 species of tribe Phyllanthae. Ancestral area estimations were performed using the BioGeoBears package as implemented in RASP and the R package 'Bamm' was used to study shifts in species diversification rates. Tribe Phyllanthae originated during the Late Palaeocene close to the Palaeocene-Eocene Thermal Maximum, but we were unable to reconstruct the origin of this group. Fossil evidence from the Eocene in Europe together with the wide distribution of early diverged taxa could hint at a boreotropical origin with early dispersals to Africa, Asia and North America. We detected multiple dispersal events within and between the major clades of tribe Phyllanthae. These occurred sometimes at similar time intervals, which coincide with known dispersal routes, but many dispersal events support an explanation through long-distance dispersal. Species diversity of tribe Phyllanthae is unevenly

distributed among clades and a pollination mutualism involving moths has not lead to increased speciation rates in all associated taxa possibly because differences in dispersal vectors might have been a limiting factor.

Keywords: BEAST, boreotropics, diversification rate shifts, *Glochidion*, *Phyllanthus* subgenus *Gomphidium*, molecular dating, Phyllanthae, pollination mutualism

Introduction

Intercontinental disjunctions associated with pantropical plant lineages have been the subject of many studies that generated different explanations with varying biogeographical implications in nonconcurrent timeframes. The presence of older taxa that occur predominantly in the southern hemisphere have been attributed to vicariance driven by plate tectonics after the break-up of Gondwana in the Jurassic (Raven & Axelrod 1974; Nelson & Platnick 1981; Wiley 1988; Humphries & Parenti 1999; Givnish & Renner 2004). Indications from micro- and macrofossil evidence from the Eocene of Europe and North America, have generated the theory of the boreotropical forests (Wolfe 1975; Tiffney 1985). A hypothesized tropical belt in the Northern hemisphere in the Early Eocene during the Paleocene-Eocene Thermal Maximum (PETM), which is supported by fossil evidence (Wolfe 1975). Subsequent cooling in the Late Eocene shifted the tropical belt closer to the equator, causing plant taxa to disperse and become isolated in Africa, Asia and North America (Wolfe 1975; Zachos et al. 2001). Boreotropical patterns have also been observed in plant clades such as Annonaceae (Thomas et al. 2015), Burseraceae (Weeks et al. 2005), Urticaceae (Huang et al. 2019) and the fern genus *Diplazium* Sw. (Wei et al. 2015). However, the boreotropical hypothesis does not account for post-Eocene dispersal events, which have sometimes been explained in the context of the Miocene geodispersal hypothesis (Zhou et al. 2012; van Welzen et al. 2014a), the Antarctic land-bridge between Australia and South America (van den Ende et al. 2017) or long-distance dispersal (Renner et al. 2001). Pantropical taxa present a valuable study subject to evaluate these theories.

The former pantropical plant genus *Phyllanthus* s.l. contained more than 800 species that were organized in eighteen morphologically defined subgenera (Bouman et al. 2018). However, this high species number is not equally distributed among all subgeneric groups and a radiation in some specific groups has been linked to the presence of mutualistic moths as pollinators (Kato et al. 2003; Kawakita & Kato 2004a; Kawakita & Kato 2009). The genus was found to be paraphyletic and nested within it were the Australasian genera *Breynia* J.R.Forst. & G.Forst., *Glochidion* J.R.Forst. & G.Forst. and *Synostemon* F.Muell. (Kathriarachchi et al. 2006; Pruesapan et al. 2012; Bouman et al. 2020; Falcón et al. 2020). If combined, *Phyllanthus* s.l. would be a giant genus with more than 1200 species (Hoffmann et al. 2006; van Welzen et al. 2014b). Recent revisions have proposed to split the genus into 10 morphologically distinguishable and monophyletic

Chapter 9

genera (Bouman et al. 2022), a summary of the new classification is shown in table 9-1. Here we discuss the various taxa according to the new classification while mentioning their treatment in the previously broader definition of *Phyllanthus*.

The species of *Phyllanthus* s.l. are characterized by small unisexual flowers with only sepals, usually nectar disc/glands and many species possess a specialized branching system called phyllanthoid branching (Webster 1956). Species with phyllanthoid branching have their axes specialized in orthotropic branches where the leaves are reduced to scales (cataphylls) and the plagiotropic branchlets are deciduous and they bear laminate leaves (Webster 1956). Several dispersal strategies have been inferred from morphological characters of the seeds and fruits in tribe Phyllanthae. The fruits and seeds are variable and are often diagnostic for specific genera or clades. The majority of fruits are dehiscent capsules that do not require additional dispersal vectors. In a few clades, dispersal by animals (probably birds) is more likely, such as with the bright blue sarcotestal seeds of *Margaritaria* L.f. (Webster 1979) or the berries of *Kirganelia* A.Juss. (*Phyllanthus* subgenus *Kirganelia*, Brunel 1987). Dispersal by large animals is largely unexplored, but could be present in a few species with larger, more indehiscent fruits such as those found in *Cicca* L. (specifically section *Omphacodopsis* (Jean F.Brunel) R.W.Bouman) and possibly in *Embllica* Gaertn. (Prasad et al. 2006). Considering the broader treatment of *Phyllanthus* s.l., this clade has a distribution traditionally attributed to Gondwanan origins, but dated reconstructions suggest that the group originated in the Early Eocene (Kawakita & Kato 2009; Luo et al. 2011; Kawakita et al. 2019). Dispersal events must therefore have occurred after the break-up of Gondwana, but there are few studies that focus on the distribution of *Phyllanthus* s.l. (for a pre-molecular analysis, see Holm-Nielsen 1979). Cai et al. (2019) also found many whole-genome duplication events in the Malpighiales with the majority occurring during the Paleocene-Eocene transition. Although sampling for some families was limited, these genome duplications were hypothesized to be related to subsequent survival under climate change and adaptation to new conditions.

Fossils of *Phyllanthus* s.l. or Phyllanthaceae are scarce, but findings in Asia include Eocene wood (Mehrotra et al. 2010), leaves (Srivastava & Mehrotra 2014; Shukla et al. 2016), pollen (Hofmann et al. 2019) and possibly Cretaceous fruits (Kapgate et al. 2017). Findings from palynological studies from the Early Eocene of Europe at the end of the PETM also found pollen attributed to tribe Phyllanthae (Gruas-Cavagnetto & Köhler 1992; Hofmann et al. 2015; Hofmann & Gregor 2018). Leaf imprints, wood or incomplete fruits and seeds remain difficult to assign with certainty to any specific clade of tribe Phyllanthae due to a lack of diagnostic characters (van Welzen et al. 2015).

Several dispersal events can already be deduced from the molecular phylogeny (see Bouman et al. 2020; Falcón et al. 2020), but have not been studied in a historical and biogeographical context. The aims of this present paper are: (1) to date the existing phylogeny and provide a more detailed exploration than

Table 9-1. Classifications of *Phyllanthus* s.l., left as previously treated as a paraphyletic genus with 17 subgenera (*P.* subgenus *Cyclanthera* (G.L.Webster) G.L.Webster was transferred as a section to *P.* subgenus *Xylophylla* (Hidalgo et al. 2020), while *P.* section *Lysiandra* was shown to be distinct from *P.* subgenus *Phyllanthus* (Bouman et al. 2021), right following the new classification as presented in Bouman et al. (2022). The numbering of the clades as in Fig. 9-2.

Clade	Taxa of <i>Phyllanthus</i> s.l.	New classification sensu Bouman et al. 2022 (genera)
A	<i>Phyllanthus</i> subgenus <i>Isocladius</i>	<i>Nellica</i>
B1	<i>Phyllanthus</i> subgenus <i>Macraea</i>	<i>Cathetus</i> subgenus <i>Macraea</i>
B2	<i>Phyllanthus</i> subgenus <i>Ceramanthus</i>	<i>Cathetus</i> subgenus .
C1	<i>Phyllanthus</i> subgenus <i>Kirganelia</i>	<i>Kirganelia</i>
C3	<i>Phyllanthus</i> section <i>Lysiandra</i>	<i>Lysiandra</i>
C4	<i>Phyllanthus</i> subgenus <i>Eriococcus</i>	<i>Nymphanthus</i>
D1	<i>Phyllanthus</i> subgenus <i>Tenellanthus</i>	<i>Moeroris</i> subgenus <i>Tenellanthus</i>
D3	<i>Phyllanthus</i> subgenus <i>Swartziani</i>	<i>Moeroris</i> subgenus <i>Swartziani</i>
D4	<i>Phyllanthus</i> subgenus <i>Afroswartziani</i>	<i>Moeroris</i> subgenus <i>Moeroris</i>
E2	<i>Phyllanthus</i> subgenus <i>Conami</i>	<i>Phyllanthus</i> subgenus <i>Conami</i>
E4	<i>Phyllanthus</i> subgenus <i>Phyllanthus</i>	<i>Phyllanthus</i> subgenus <i>Phyllanthus</i>
E5	<i>Phyllanthus</i> subgenus <i>Xylophylla</i>	<i>Phyllanthus</i> subgenus <i>Xylophylla</i>
F1	<i>Phyllanthus</i> subgenus <i>Anesonemoides</i>	<i>Cicca</i> subgenus <i>Anesonemoides</i>
F1	<i>Phyllanthus</i> subgenus <i>Pseudogomphidium</i>	<i>Cicca</i> subgenus <i>Menarda</i>
F1	<i>Phyllanthus</i> section <i>Cicca</i> , <i>Polyanthes</i> & <i>Ompheocodopsis</i>	<i>Cicca</i> subgenus <i>Cicca</i>
F1	<i>Phyllanthus</i> subgenus <i>Betsileani</i>	<i>Cicca</i> subgenus <i>Betsileani</i>
F2	<i>Phyllanthus</i> subgenus <i>Gomphidium</i>	<i>Dendrophyllanthus</i>
G	<i>Phyllanthus</i> subgenus <i>Emblica</i>	<i>Emblica</i>
H	<i>Phyllanthus</i> subgenus <i>Phyllanthodendron</i>	<i>Glochidion</i> subgenus <i>Phyllanthodendron</i>
H	<i>Glochidion</i>	<i>Glochidion</i>
I	<i>Synostemon</i>	<i>Synostemon</i>
J	<i>Breynia</i>	<i>Breynia</i>

Chapter 9

previous studies; (2) to analyse the historical biogeography of the genera in tribe Phyllanthae that made up *Phyllanthus* s.l.; and (3) to explain the speciation-distribution of the various clades and to assess the evidence for of pollinator related diversification.

Materials and methods

Sampling of tribe Phyllanthae

In this study we used a subset of the datasets employed in Bouman et al. (2021), which presents the largest sampling of *Phyllanthus* s.l. to date. To limit the extent and possible effects of missing data, we used the reduced dataset where we had genetic information for each accession with a minimum of 3500 nucleotides out of 5500. Species present with multiple samples in Bouman et al. (2021) are here limited to include only one accession, except for the *P. virgatus* complex where samples of Australia were retrieved in a different clade from those in Asia (presumed here to be *P. simplex*). The trimmed dataset contains 21 species of *Breynia*, four species of *Synostemon*, five species of *Glochidion*, four species of *Margaritaria* L.f., one species of *Flueggea* Willd. and 173 species of *Phyllanthus* s.l. *Leptopus chinensis* (Bunge) Pojark. and *Notoleptopus decaisnei* (Benth.) Vorontsova & Petra Hoffm. of tribe Poranthereae were used as an outgroup for tribe Phyllanthae. Almost all genera of the tribe were included except *Heterosavia* (Urb.) Petra Hoffm. and *Lingelsheimia* Pax as we did not have the full set of markers for any species from these genera. The sampling for *Phyllanthus* s.l. covers all reinstated genera (Table 9-1), the majority of sections and most of its distribution. Some geographical areas like India and the Neotropics are not well represented in this dataset and should be expanded upon in future studies.

Dating

A two-step approach was implemented to date the molecular phylogeny of *Phyllanthus*. In the first step, the molecular dataset presented by Kathriarachchi et al. (2005) and dated by Kawakita & Kato (2009) was re-calibrated with one additional fossil calibration point (see below) to obtain a base for the divergence time between tribe Phyllanthae and tribe Poranthereae (see supplementary table 9-1 for Genbank numbers). Outgroups were taken from the closest related family, the sister family Picrodendraceae (Xi et al. 2012). The dataset of Kathriarachchi et al. (2005) used the molecular markers *PHYC*, *atpb*, *matK* and *ndhF* and we therefore did not combine this with the dataset of Bouman et al. (2020), which consists of the molecular markers ITS, *PHYC*, *accD-psaI*, *matK* and *trnS-trnG*. In the second step, we implemented the divergence time between tribe Phyllanthae and tribe Poranthereae as a secondary calibration as indicated by the phylogeny of the Phyllanthaceae (Supplementary figure S9-1).

The molecular phylogeny of tribe Phyllanthae was dated using BEAST v. 1.10.4 (Suchard et al. 2018). The input file was prepared using BEAUTI v. 1.10.4

(within the BEAST package). MrModeltest v.2 (Nylander 2004) was used to obtain the best-fitting model according to the lowest Akaike Information Criterion (AIC) for each marker, selecting the same model for all markers. Substitution rates were calculated under the General Time Reversal (GTR) model with a discrete Gamma distribution (, 4 categories of evolutionary rates among sites and a certain number of invariable sites (+I). Divergence times were estimated using an uncorrelated relaxed clock model (Drummond et al. 2007) with an exponential distribution of rates and the Yule process was selected as a tree prior (Yule 1925; Gernhard 2008) and a random starting tree was used. Two independent runs were done, each with 220 million generations of Markov Chain Monte Carlo (MCMC) and trees were sampled every 22,000 generations. Effective Sampling Sizes (ESS), representing the convergence of the two runs, were checked in Tracer v. 1.7.1 (Rambaut & Drummond 2018), while the Maximum Clade Credibility (MCC) tree for each run was checked for topological differences before combining the tree files using Logcombiner v.1.10.4 (part of the BEAST package) with a burnin of 20 % per tree file. TreeAnnotator v.1.10.4 (within the BEAST package) was used to find the MCC tree and this was visualized using Figtree v.1.4.3 (Rambaut 2014). Our analyses of divergence times were estimated using several fossils as calibration points. These were set as priors for specific taxon groups with an exponential distribution:

1. An Early Eocene calibration with a median age of 52.2 MA was put as offset for the prior with an exponential distribution and a mean of 1.5 to allow for older ages for the clade comprising *Flueggea* and *Phyllanthus* s.l. including *Glochidion*, *Breynia* and *Synostemon*. Fossil 3-colporate pollen of the Early Eocene (c. 47–56 Ma) Woolwich bed in Kent, England, was determined to be related to *Flueggea* or *Phyllanthus* (Gruas-Cavagnetto & Köhler 1992; Sagun & van der Ham 2003). Additional findings of *Flueggea*-type pollen from London (also Woolwich formation) and the Knopffeld formation in Austria from the Early Eocene (Hofmann et al. 2015) provided further support for this calibration point. The Woolwich bed finding has been used as a calibration point by Kawakita & Kato (2009), Luo et al. (2011b) and van Welzen et al. (2015). Older fruits from the Late Maastrichtian (66–72) Ma of India have been suggested to be related to the genus *Phyllanthus*, but could not be assigned with full certainty as fruits are notoriously difficult and there was no exhaustive comparison with fruits of other genera within the Phyllanthaceae family (Kapgate et al. 2017). Therefore we have opted to not include this in our analysis.
2. Leaf impressions tentatively assigned to *Glochidion* from the Middle Miocene (c. 11.6 Ma with a mean of 1.5) of India (Prasad 1994; Antal & Prasad 1996) were used as an offset minimum age constraint for Clade H, which contains *Glochidion* (also used in Kawakita & Kato 2009).
3. Recent findings of pantoporate pollen from the Changchang Formation

Chapter 9

(Hainan Island, South China) have been attributed to *Phyllanthus* s.l. (Hofmann et al. 2019). The material is estimated to be of late Early Eocene (Bartonian, 37.8–48 Ma; Aleksandrova et al. 2015). This specific pollen type can be found in *Nymphanthus* Lour. (*Phyllanthus* subgenus *Eriococcus*) and subgenus *Ceramanthus* (listed as subgenus *Isocladus* section *Ceramanthus* in Hofmann et al. 2019, here listed in table 9-1 as *Cathetus* Lour.), but pollen sizes were more similar to those found in the latter. Therefore, this was used as an offset fossil calibration point for the clade comprising the sister groups *Phyllanthus* subgenus *Ceramanthus* and subgenus *Macraea* (*Cathetus*, Fig. 9-2; clade B) and the offset was set to 37.8 Ma with a mean of 1.5.

4. The stem age for the analysis of our dataset of tribe Phyllantheae was calibrated using divergence time estimates with tribe Poranthereae and Wielandiaeae taken from our analysis of the Phyllanthaceae family dataset and compared to Kawakita et al. (2009). The node was calibrated using an offset of c. 75 Ma with a mean of 1.5 to allow for older ages (see supplementary Fig. 9-1)

Additionally, to date the family Phyllanthaceae other calibration points similar to those implemented in Kawakita & Kato (2009) were implemented as an offset.

5. *Bischofia* pollen from the Middle Eocene (37.2–41.2 Ma) also from the

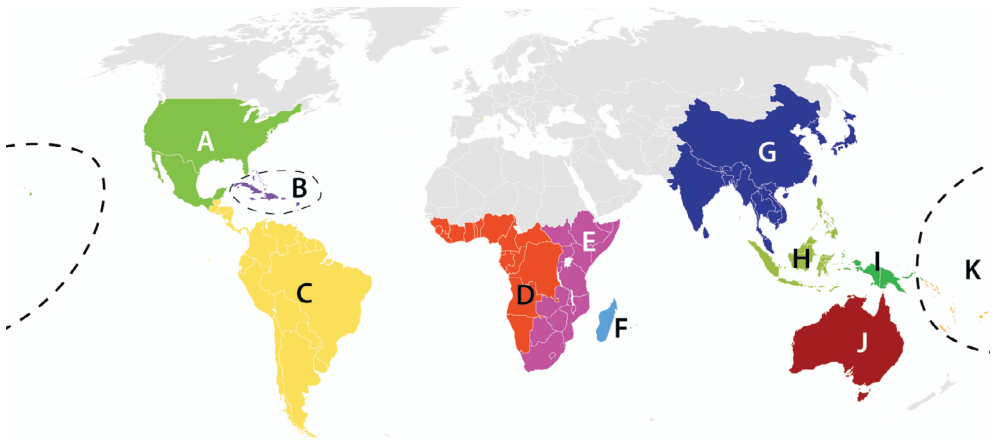


Figure 9-1. Map with biogeographical regions as specified for this study of Tribe Phyllantheae: A, North America to Mexico; B, West Indies; C, South America and part of the Panama Isthmus; D, West Africa with eastern border following Namibia, Democratic Republic of Congo and Central African Republic; E, South and Eastern Africa; F, Madagascar and the Mascarene Islands; G, mainland Asia stretching from India to Peninsular Malaysia; H, W. Malesia including Philippines; I, E. Malesia (mainly Papua New Guinea); J, Australia; K, Pacific Islands.

- Woolwich formation in England was used as a minimum age constraint for the subfamily Antidesmatoidea (Gruas-Cavagnetto & Köhler 1992 as implemented in Kawakita & Kato 2009).
6. The clade containing tribe Poranthereae and tribe Wielandieae (sensu Hoffmann et al. 2006) was constrained with a calibration point based on *Actephila* Blume pollen type from the Late Eocene (median 33.9 Ma) of France (Gruas-Cavagnetto & Köhler 1992 as implemented in Kawakita & Kato 2009).
 7. The stem age for the split between Phyllanthaceae and Picrodendraceae was conservatively set to 80 Ma based on molecular dating from Xi et al. (2012). Similar age estimates, but with varying 95% Highest Posterior Density (HPD) intervals have been obtained by Magallon et al. (2015), Davis et al. (2005) and Li et al. (2019). Kawakita & Kato (2009) opted to use the occurrence of Eudicot pollen as the root age for their phylogeny. As this is unlikely, since Phyllanthaceae occurred later, we decided to use the base estimate from the former papers.

Ancestral range estimation

Eleven biogeographical areas were specified based on levels of species endemism and tectonic history (Fig. 9-1). Distributions of the various species were taken from various monographs and floras (e.g. Webster 1956, 1957, 1958; Airy Shaw 1975, 1980; Bouman et al. 2018). The biogeographic area that covers islands in the Pacific Ocean covers mostly New Caledonia with over 100 endemic species of *Dendrophyllanthus* S.Moore (*Phyllanthus* subgenus *Gomphidium*). However, to not create separate areas for other islands, we also include islands from the rest of the Pacific. Most discussions below focus on New Caledonia unless specified otherwise.

The MCC tree resulting from our BEAST analysis was trimmed by excluding the outgroups of tribe Phyllanthae. Ancestral Range estimations were performed using RASP (Reconstructed Ancestral State in Phylogenies) 4.2 (Yu et al. 2015, 2020). We tested for different models for biogeographic inferences using the R package 'BioGeoBears' as implemented in RASP (Matzke 2013a, 2014). These were the S-Diva model (called Divalike in 'BioGeoBears'), DEC and BAYAREA (BAYAREALIKE), which is based on the likelihood of a given history and takes into account the relative probability of each biogeographic change and waiting times between events in a Bayesian framework (Landis et al. 2013). With the S-Diva model, the frequencies of ancestral ranges of specific nodes is averaged over all trees while alternative ranges are weighted by their frequency and node occurrence (Yu et al. 2010). 'BioGeoBears' additionally tests whether these models show a different/better fit when the founder effect (+J) is taken into account (Matzke 2013b, 2014). Usage of the founder effect as implemented by 'BioGeoBears' has recently been cautioned by Ree & Sanmartín (2018).

Dispersal constraints were defined for four time periods based on the

Chapter 9

geological history of the various continents involved. Dispersal constraints were defined similarly to those implemented by Buerki et al. (2011), Wei et al. (2015) and Thomas et al. (2015). These were mostly defined based on distance, but had a correction for specific land bridges and were categorized as very low dispersal = 0.01; low dispersal = 0.25; medium dispersal = 0.5; moderate dispersal = 0.75; high dispersal and adjacent areas = 1.0 (see Supplementary table 9-2). We allowed for 2–3 areas per node, as higher numbers gave far longer computation times with more ambiguous results. The model selection from BioGeobears, retrieved the highest Akaike Information Criterion (AIC) and weighted AIC score for the BAYAREALIKE model and DEC model (Table 9-2). BiogeoBears is able to compare the various models, but also incorporates a possible founder effect (+J). A likelihood Ratio test (LRT) was used to see if incorporating the founder effect gives a significantly different result. Table 9-2 shows a significant ($P < 0.05$) result for the comparisons DEC/DEC+J and BAYAREALIKE/BAYAREALIKE+J. The null hypothesis that the standard model and the model+founder effect show similar likelihoods for our data is therefore rejected and the analysis including the founder effect is omitted here as it has a lower AIC score.

Estimating and comparing speciation rates and identifying shift rates

To determine whether diversification rates differed per clade and could be associated with any specific ecological variable, we used BAMM v. 2.5 (Rabosky 2014) and the R package BAMMtools v. 2.1 (Rabovsky et al. 2014). In this method different models are fitted to the MCC tree to explore shifts in diversification rates. Speciation rates were calculated on the trimmed MCC tree and priors were adjusted to the scaling of our trees by using the command "setBAMMpriors". Differences in sampling number were adjusted for each clade according to the estimated number of species per subgenus (corrected with latest taxonomic findings sensu Bouman et al. 2020; Falcón et al. 2020). Rounded global sampling fractions for each clade were: *Nellica* Raf. 20%, *Cathetus* Lour. 40%, *Kirganelia* A.Juss. 54%, *Nymphanthus* 20%, *Lysiandra* ((F.Muell.) R.W.Bouman, I.Telford & J.J.Bruhl 41%, *Moeroris* Raf. 20 %, *Phyllanthus* s.s., the Neotropical clade 30%, *Dendrophyllanthus* 10%, *Cicca* 44%, *Emblica* 23%, *G.* subgenus *Phyllanthodendron* ((Hemsl.) R.W.Bouman) and *Glochidion* subgenus *Pseudoactephila* (Croizat) R.W.Bouman 10%, *Glochidion* 1.4%, *Synostemon* 10% and *Breynia* 25% (see table 9-1 for names under *Phyllanthus* s.l.). Initial runs indicated high speciation rates for *Glochidion*, so additional analyses were run with sampling of *Glochidion* set to 5% and 10% to compare overshadowing of signals. The MCMC was run for 10,000,000 generations and was saved every 1000 generations. Expected number of shifts was set to 3. A burn-in of 10% was discarded and Effective Sampling Sizes (ESS) were determined by using the Coda Package for R (Plummer et al. 2006). The output was further analysed using BAMMtools to determine the single best shift configuration and the maximum shift credibility configuration. Independent speciation rates for the various clades (Fig.

Table 9-2. Model comparison from BioGeoBears showing lognormal likelihood (LnL), Akaike Information Criterion (AIC) and weighted AIC (AICwt) and comparison to incorporation of founder effect. Founder effect is tested using the Likelihood Ratio Test.

	LnL	numparams	d	e	j	AICc	AICc_wt	LRT test
DEC	-428,7	2	0,0052	1,00E-12	0	861,5	7,70E-11	
DEC+J	-408,8	3	0,0035	1,00E-12	0,02	823,7	0,013	2,60E-10
DIVALIKE	-425,2	2	0,0059	1,00E-12	0	854,5	2,60E-09	
DIVALIKE+J	-415	3	0,0042	1,00E-12	0,015	836,1	2,50E-05	6,30E-06
BAYAREALIKE	-483,1	2	0,004	0,034	0	970,2	2,00E-34	
BAYAREALIKE+J	-404,4	3	0,0021	0,004	0,025	815	0,99	4,50E-36

Chapter 9

9-2: clades A–J while separating C1, C3, C4, F1 & F2) were also extracted in R.

Results

Divergence time estimation

Our reconstruction of *Phyllanthus* s.l. and related genera indicate that the clade originated sometime during the Late Paleocene or Early Eocene. The MCC tree resulting from BEAST for the Phyllanthaceae had generally high node support (Supplementary Fig. 9-1). Node support was only a bit lower within a few genera and within the subfamily Antidesmatoideae between genera (PP>0.74). Despite differing constraints on the divergence node between Picrodendraceae and Phyllanthaceae, both family-level analyses resulted in an estimated age for the divergence between tribe Phyllantheae with tribe Wielandieae and Poranthereae around 75 Ma (HPD 94–63 MA; Supplementary Fig. 9-1). This resulted in our setting of 75 as a median age for the stem age of our analysis of *Phyllanthus* s.l. and the other genera.

The phylogeny focusing on *Phyllanthus* s.l. and related genera showed no major topological differences with previous analyses (Fig. 9-2). Additional age estimations in BEAST while excluding the calibration point for the genus *Glochidion* (based on Prasad 1994; Antal & Prasad 1996), did not result in significant changes to age estimations of this (12.41 Ma; Table 9-3) and other clades. Placing the fossil calibration point of pantoporate pollen (Aleksandrova et al. 2015) as the crown age of *Nymphanthus* instead of *Cathetus* resulted in slightly older nodes for the outgroups, *Nellica* (Clade A) and *Cathetus* (Clade B), but with lower ESS scores. The crown age of tribe Phyllantheae was dated to c. 60 Ma (HPD 53.45–72.38 Ma) (Fig. 9-2). The crown age of Clade C, which corresponds here to *Kirganelia*, *Nymphanthus* and the Australian "*Lysiandra* clade" is estimated to be around 36 Ma (HPD 28.83–45.08). Similarly the crown age of Clade D ("large African" clade) and Clade E (Neotropical clade) are 34.44 Ma (HPD 27.30–41.87) and 32.01 Ma (HPD 24.65–39.34), respectively. Clade F can be divided into two major taxonomical subclades: F1 which corresponds to *Dendrophyllanthus*; F2 which corresponds to the reinstated genus *Cicca* L., which contains several sections and subgenera from *Phyllanthus* s.l. (Table 9-1). Clade F1 includes species from a multitude of areas and the crown age is estimated to be 27.69 Ma (HPD 19.71–35.76). The crown age of *Embllica* (node G) was inferred to be 18.7 Ma (HPD 10.98–26.50). The genera *Glochidion* (including *P.* subgenus *Phyllanthodendron*), *Breynia* and *Synostemon* are estimated to have diverged from other species of *Phyllanthus* s.l. in the Late Oligocene/Early Miocene at 26.24 Ma (HPD 19.34–38.44).

Ancestral area estimation

Node 1 and 2 (Fig. 9-2) were omitted from the biogeographic analysis as outgroups were removed. While nodes 9–11 show medium support for an ancestral area in mainland Asia, support for nodes 3–8 is generally low and could only infer a wide

ancestral area for *Phyllanthus* s.l. Node 3 (common ancestor of *Phyllanthus* s.l. + *Glochidion* + *Breynia* + *Synostemon*) was inferred to be Africa, Mainland Asia or Australia by BAYAREA (PP 0.33) while DEC indicated a wider area of North America, Eastern Africa and mainland Asia (Relative Probability 0.33).

The ancestral area of Clade A was reconstructed to be in North America or Africa (PP = 0.20, RP = 0.35; Fig. 9-2). Both BAYAREALIKE and DEC indicate an ancestral area of Africa to Asia for *Cathetus* (*P.* subgenus *Cathetus* and *Macraea*, Clades B1 & B2; Fig. 9-2). Both subclades in this group show dispersal exchanges between Africa and Asia, but only *C.* subgenus *Macraea* has species present in Australia.

Clade C (Fig. 9-2) consists of three major clades, which correspond respectively to *Kirganelia* (C1); *Lysiandra* (C3) and *Nymphanthus* (C4). While BAYAREALIKE reconstructed the area to be quite wide, ranging from West Africa to Asia (PP = 0.51), DEC indicated an African origin (C1 RP = 0.56) with two separate instances of dispersal events to Asia. One dispersal and speciation event into Madagascar is found in *Kirganelia* in both analyses. *Lysiandra* consists of species occurring only in Australia, which is consistent with a single dispersal and subsequent speciation event found for node C3 (PP = 0.72, RP = 1). *Nymphanthus* is inferred to have originated in mainland Asia (C4 PP = 0.45, RP = 0.73) with two independent dispersals to Malesia and further.

The ancestral area of *Moeroris* (*P.* subgenus *Tenellanthus*, *Swartziani* and *Afroswartziani*, Clade D) is estimated to be in Africa (BAYAREALIKE: DE, PP = 0.46; DEC: D, RP = 0.39; Fig. 9-2). The majority of species are distributed in Africa, but we find one dispersal event to North America (*M. aranaria* (A.Gray) R.W.Bouman) and one to South America (*Moeroris stipulata* Rafinesque) and dispersal event to Madagascar (Fig. 9-2).

The large Neotropical clade (E), consisting of *Phyllanthus* subgenus *Phyllanthus*, *Conami* (Aubl.) G.L.Webster and *Xylophylla* (L.) Pers., is inferred to have originated in South America (node E, PP = 0.27; DEC: AC, RP = 0.98; Fig. 9-2). Some species of *P.* subgenus *Phyllanthus* are currently found in North America. Within subgenus *Xylophylla* we find an exchange between South America and the Carribean, but we were unable to reconstruct the ancestral area for this.

The ancestral area of the speciose genus *Dendrophyllanthus* (F2) is inferred to be Australia (PP = 0.65, RP = 0.74) and it gave rise to independent dispersals to New Caledonia in both subclades (Fig. 9-2). One clade contains two independent dispersals from Australia to Papua New Guinea. The ancestral area of *Cicca* (F1) is inferred to be in Madagascar with one lineage (*corresponding to C.* subgenus *Cicca*) subsequently dispersing to Africa and South America.

Emblica (G), and the genera *Glochidion* (H), *Synostemon* (I) and *Breynia* (J), were reconstructed to have an ancestral area in mainland Asia, with for *Synostemon* a single dispersal event to Australia.

Chapter 9

Table 9-3. Summary of the dated phylogeny and ancestral area reconstruction for major clade nodes following figure 9-2. Shown are for each major node node the posterior probabilities, mean ages of the nodes, 95% height of the Posterior Density intervals, BAYAREA reconstruction with next to it the Posterior Probability and DEC with relative probability.

Node label	Posterior	Age	95% HPD	Bayarea	PP	DEC	RP
1	0,58	60,51	72.38-53.45				
2	1	55,11	61.36-53.00				
3	0,98	51,79	58.36-46.00	DGJ	0,3255	AEG	0,3286
4	1	48,74	55.09-42.78	DGJ	0,3369	G	0,4675
5	1	44,64	51.24-38.17	DGJ	0,3247	G	0,2325
6	1	38,84	45.54-32.22	DEG	0,2293	A	0,1134
7	0,99	35,48	42.47-28.86	DG	0,1774	ACJ	0,1453
8	0,91	32,75	39.62-25.66	G	0,2281	J	0,4717
9	1	26,24	33.44-19.34	G	0,6	G	0,9155
10	1	22,13	28.59-16.32	G	0,6576	G	0,5304
11	1	16,95	22.99-11.80	G	0,5834	GJ	0,7594
A	1	22,66	41.25-9.05	AE	0,2049	AEG	0,3526
B	1	38,17	41.16-37.20	DG	0,3682	G	0,3432
B1	1	25,72	34.27-17.14	DG	0,5034	DG	0,9719
B2	1	13,5	25.58-5.32	DG	0,7446	DG	1
C	1	36,84	45.08-28.83	DGJ	31,02	G	0,5763
C1	1	21,24	36.01-9.87	DG	0,5147	D	0,5557
C2	1	29,58	38.12-21.93	G	0,3519	GJ	0,5531
C3	1	23,62	31.62-15.72	J	0,7152	J	1
C4	1	23,74	31.88-16.28	G	0,451	G	0,7299
D	1	34,44	41.87-27.30	DE	0,4641	D	0,3933
D1	1	21,32	33.45-10.24	DE	0,7973	D	0,4275
D2	0,95	31,7	39.06-24.56	DE	0,6249	AD	0,2895
D3	1	19,83	30.83-9.81	DE	0,7246	AD	0,4768
D4	1	27,4	34.32-21.07	DE	0,8499	E	0,6935
E	0,99	32,01	39.34-24.63	C	0,2731	AC	0,9773
E1	1	29,48	36.74-22.50	C	0,4156	C	0,9867
E2	0,57	21,32	31.34-11.75	C	0,6525	C	0,6188
E3	0,4	28,09	35.38-21.46	C	0,3893	C	0,7495
E4	0,47	26,21	34.10-19.12	C	0,3853	C	0,9812

Historical biogeography of tribe Phyllantheae

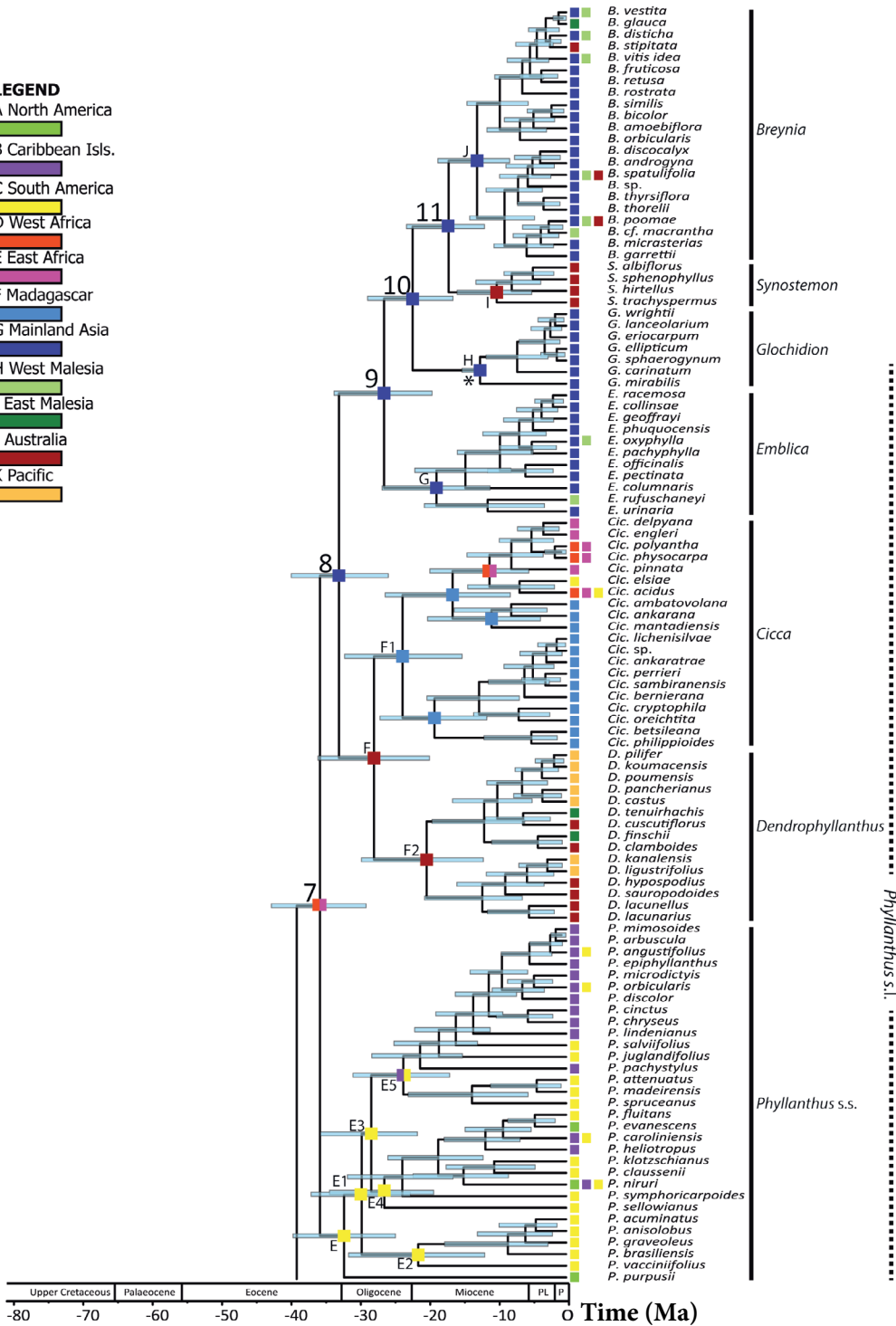
E5	1	23,47	30.72-16.81	BC	0,5265	BC	0,9842
F	0,66	27,69	35.76-19.72	J	0,1184	FJ	0,7084
F1	1	23,58	31.92-15.02	F	0,5128	F	0,6396
F2	1	20,11	29.49-11.96	J	0,6532	J	0,7425
G	1	18,7	26.42-10.98	GH	0,8815	GH	0,6422
H	1	12,41	14.10-11.60	G	0,9435	G	1
I	1	12,84	18.48-8.17	G	0,965	G	0,9924
J	1	10,02	15.70-4.98	J	0,8953	J	1

Figure 9-2. Chronogram (MCC tree) of tribe Phyllantheae generated via Bayesian analysis in BEAST. Axis scaled to node ages and with designated time periods according to International Commission on Stratigraphy (ICS) V. 2020/03. Calibration points are indicated with *, major nodes are numbered 1–11 while clades follow A–J as discussed in text. Ancestral area estimation as inferred from the BAYAREALIKE model from BiogeoBears given for selected nodes in squares with legend for the different areas, colours correspond to map of figure 1. A broader definition of *Phyllanthus* from previous classifications is shown with a dotted line on the right. Figure shown on following two pages

Chapter 9

LEGEND

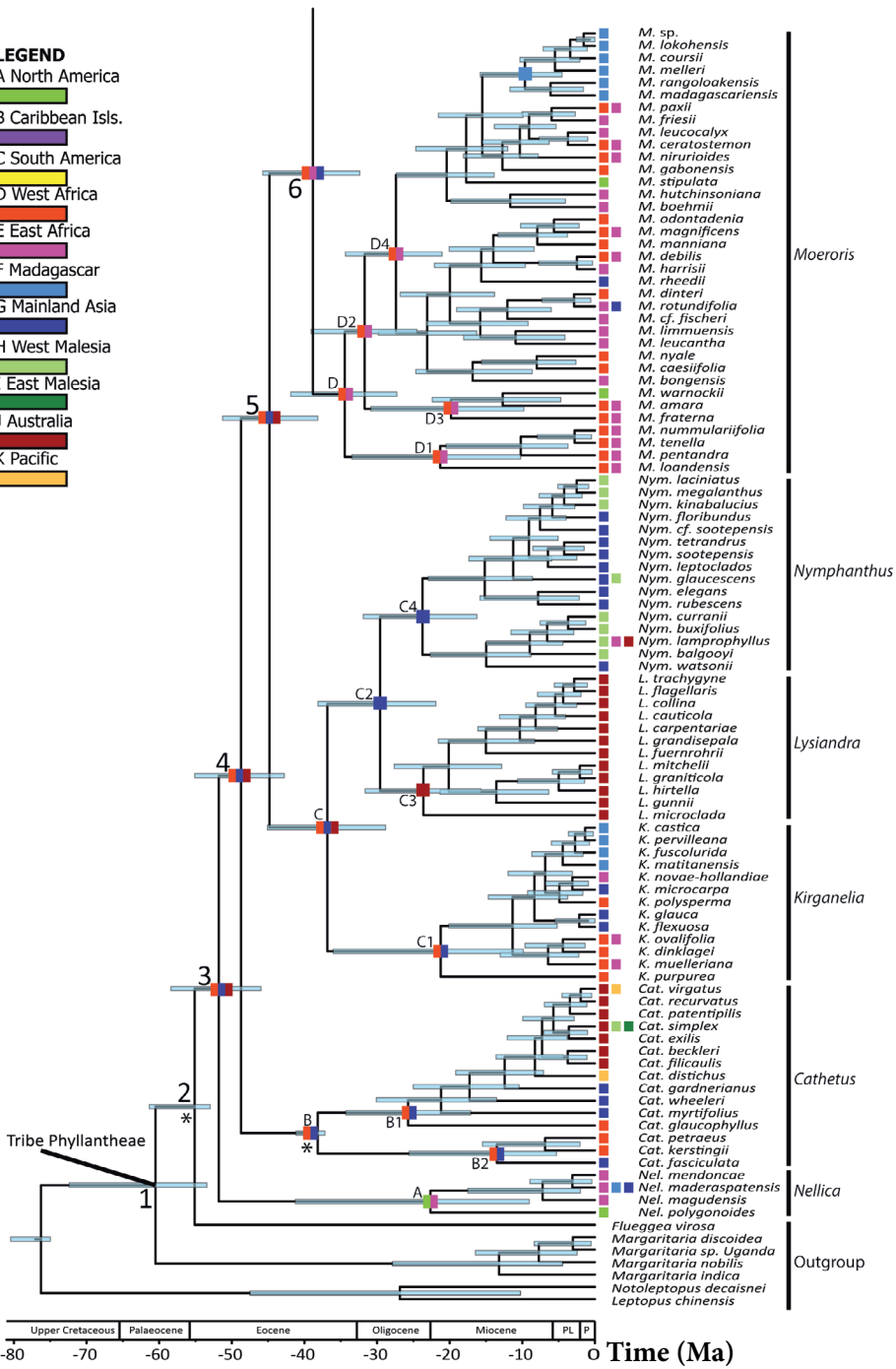
- A North America
- B Caribbean Isls.
- C South America
- D West Africa
- E East Africa
- F Madagascar
- G Mainland Asia
- H West Malesia
- I East Malesia
- J Australia
- K Pacific



Historical biogeography of tribe Phyllanthae

LEGEND

- A North America
- B Caribbean Isls.
- C South America
- D West Africa
- E East Africa
- F Madagascar
- G Mainland Asia
- H West Malesia
- I East Malesia
- J Australia
- K Pacific



Chapter 9

Diversification rate heterogeneity

Effective sample sizes after burnin were >600 for both the number of shifts and log likelihoods and MCMC chain convergence was confirmed. Speciation rates (λ) overall were 0.19 species/million years [95% interval 0.16–0.21] while mean extinction rates (μ) were 0.03 sp/Ma [95% interval 0.01–0.06]. Speciation rates were relatively similar between the clades of *Nellica* (Clade A) and the Neotropical Clade E at 0.15 species/Myr (Table 9-3). Extinction rates for these clades was relatively low at 0.01 species/Myr. An increase in speciation rates can be seen in Clades F–J, with highest speciation occurring in Clade H (*Glochidion*) at 0.56 species/Myr. The 95 % credible set of rate shift configurations sampled with BAMM included fifteen distinct shift configurations, mostly indicating a shift in speciation of the genus *Glochidion* (Fig. 9-3, clade H). This shift was also found by the Maximum shift credibility plot. Additional shift changes were found at node 8, which encompasses the clades with higher speciation as seen in Table 9-4. The rate-through-time plot of tribe Phyllanthae shows a steady increase from its inception, with a sudden increase in speciation rate around 10 Ma. Plots of *Kirganelia* (Clade C1) and *Cicca* (Clade F1) show a slight increase, but then decreasing of the curve. The genus *Dendrophyllanthus* (Clade F2) shows an increasing speciation rate through time, but not as drastic as observed for *Glochidion* (clade H), which is close to exponential. The rate through time plot of *Breynia* and *Synostemon* (supplementary figure 4) also show a rate higher than the mean speciation rate through time with a slight smoothing of the curve towards the present.

Discussion

Age estimates

Our reconstruction of *Phyllanthus* s.l. and related genera indicates that the clade originated sometime during the Late Paleocene or Early Eocene. The MCC tree resulting from BEAST for the Phyllanthaceae showed no major topological differences with the one presented by Kathriarachchi et al. (2005) and node support was generally high (Supplementary Fig. 1) The dated phylogeny is largely congruent with the results of previous studies (e.g. Kawakita & Kato 2009; Luo et al. 2011b; van Welzen et al. 2015), but provides a better supported backbone between the major clades of tribe Phyllanthae. The recent species-level dated phylogeny of angiosperms by Janssens et al. (2020) inferred that Angiosperms originated before the Cretaceous, which would indicate older ages for the major clades of flowering plants. Nevertheless, the crown age of tribe Phyllanthae is inferred in their study at 65.92 Ma (HPD 74.33–45.58; Janssens et al. 2020; derived from supplementary material 5), which is comparable to our results (60.51 Ma; HPD 72.38–53.45). Divergence times estimations of *Breynia* and *Synostemon* were comparable to those found in van Welzen et al. (2015). The crown age of *Breynia*, 12.84 Ma (Table 9-3; HPD 18.48–8.17) was found to be more recent than the reconstruction of van Welzen et al. (2015; 20.6 Ma), while *Glochidion* seemed older (12.41 Ma here vs 5.61

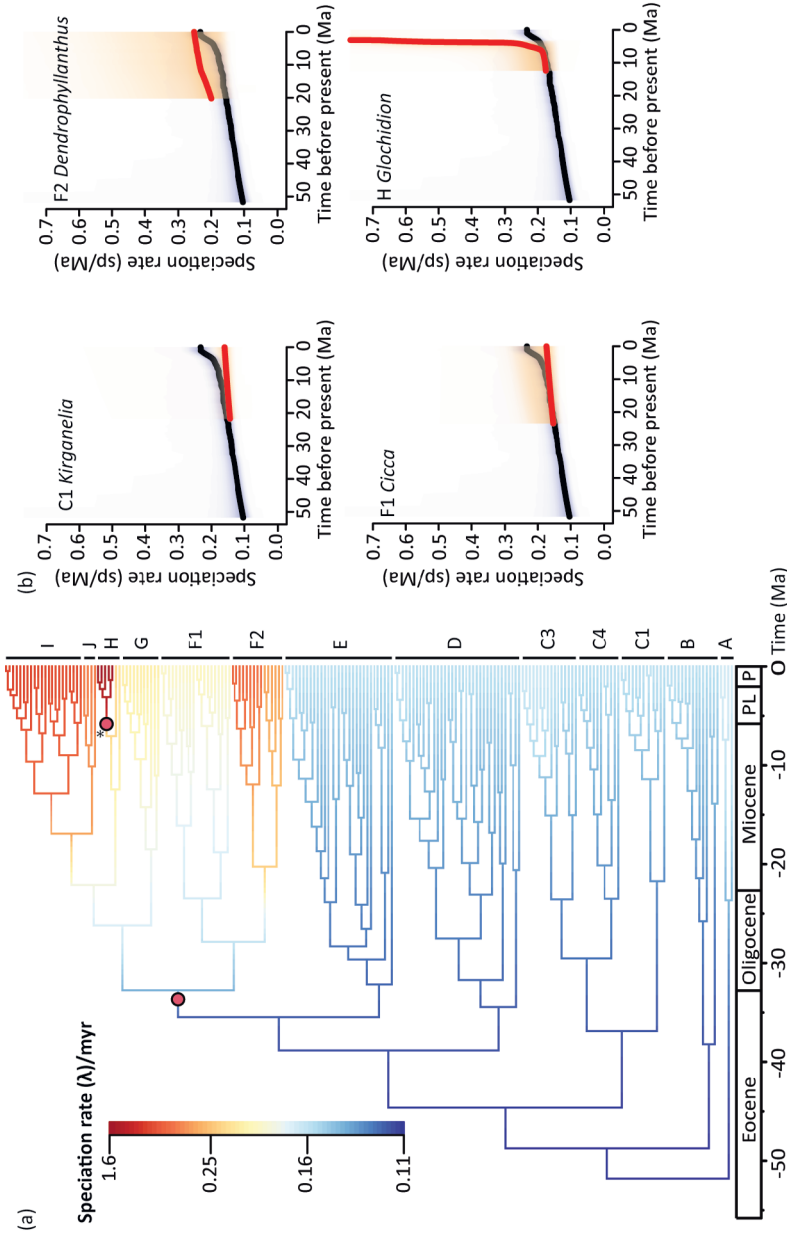


Figure 9-3. Speciation rate (λ) of *Phyllanthus*, *Glochidion*, *Bryenia* and *Synostemon*. (a) Chronogram of *Phyllanthus* with branch lengths colored according to speciation rate following Jenks bucketing. Red circles indicate shifts in speciation rates as found by the best credible shift analyses, asterisk (*) includes those found by maximum posterior shift probability. (b) Speciation rates through time of selected clades. Black line represents mean speciation rate through time of the whole phylogeny, red is of selected clade.

Table 9-4. Median speciation (λ), extinction (μ) and net diversification rates (with 95% CI) For *Glochidion*, *Breynia*, *Synostemon* and major clades within *Phyllanthus*. Clades as in Fig. 9-2.

Clade	Age	Speciation		Extinction		Net Diversification	
		Median	95% CI	Median	95% CI	Median	95% CI
All	51,79	0,18	0.16-0.21	0,02	0.01-0.06	0,16	0.15-0.16
A <i>Nellica</i>	22,66	0,15	0.12-0.19	0,01	0.001-0.10	0,13	0.09-0.12
B <i>Cathetus</i>	38,17	0,15	0.13-0.18	0,01	0.001-0.06	0,14	0.12-0.13
C1 <i>Kirganelia</i>	21,24	0,15	0.13-0.19	0,01	0.001-0.05	0,14	0.13-0.13
C2 <i>Lysiantra</i>	23,62	0,15	0.13-0.10	0,01	0.001-0.05	0,14	0.13-0.13
C4 <i>Nymphanthus</i>	23,74	0,16	0.13-0.19	0,01	0.001-0.06	0,14	0.14-0.13
D <i>Moeroris</i>	34,44	0,15	0.13-0.18	0,01	0.001-0.05	0,14	0.13-0.13
E <i>Phyllanthus</i> s.s.	32,01	0,15	0.13-0.18	0,01	0.001-0.05	0,14	0.13-0.13
F1 <i>Cicca</i>	23,58	0,17	0.14-0.28	0,01	0.001-0.06	0,16	0.21-0.14
F2 <i>Dendrophyllanthus</i>	20,11	0,24	0.15-0.56	0,02	0.001-0.34	0,22	0.21-0.15
G <i>Emblica</i>	18,7	0,17	0.14-0.30	0,01	0.001-0.08	0,16	0.22-0.14
H <i>Glochidion</i>	12,41	0,56	0.40-0.75	0,07	0.01-0.24	0,50	0.51-0.39
I <i>Breynia</i>	12,84	0,30	0.17-0.49	0,03	0.002-0.24	0,26	0.27-0.17
J <i>Synostemon</i>	10,02	0,27	0.16-0.47	0,03	0.002-0.24	0,24	0.26-0.15

Ma in van Welzen et al. 2015). This is not entirely explained by the fossil calibration point for *Glochidion*, as additional analyses without this fossil gave similar results. More likely, it is caused by a combination of including more fossil calibration points as well as a larger sampling.

Origin of Phyllanthus and related genera

Fossil pollen indicates that several taxa of tribe Phyllanthae were already present in Europe during the early Eocene and pollen attributed here to Clade B (*Cathetus*) indicates an early dispersal to China (Gruas-Cavagnetto & Köhler 1992; Hofmann et al. 2015, 2019). The pantropical genus *Margaritaria* is reconstructed to have diversified during the Middle Miocene (Fig. 9-2), but it was not used in our reconstruction of the ancestral areas. The Asian species *M. indica* (Dalzell) Airy Shaw was previously retrieved as sister to the other species from South America and Africa (Webster 1979; Bouman et al. 2021). Fossil findings from the Eocene could indicate that boreotropical migration was part of the history of *Phyllanthus* s.l. and possibly *Flueggea* Willd. and that taxa later dispersed to Asia, Africa and North America while becoming extinct in Europe. The genus *Flueggea* might have persisted in Europe as *F. tinctoria* (L.) G.L. Webster is native to Spain and Portugal (Webster 1984), while there is only one invasive species of *Phyllanthus* (*P. tenellus* Roxb. to be placed in *Moeroris* Raf.) in Europe (Crisafulli et al. 2011). Limited sampling of *Nellica* and *Flueggea*, however, prevents us from further inferences; the European species *F. tinctoria* would be especially interesting to include in future studies. The major nodes 3–5 of the backbone phylogeny of *Phyllanthus* s.l. are reconstructed to have a wide ancestral area with an unclear area of origin (Fig. 9-2). Our reconstruction shows this wide ancestral area for the nodes in the time period just after the PETC till the start of the late Eocene (38.84 Ma; HPD 45.54–32.22, Table 9-3). Species of *Nellica* (Clade A) are found in North America, Africa and Asia, which is consistent with a boreotropical origin. However, the estimate for the crown age for Clade A (22.66 Ma; HPD 41.25–9.04) shows a wide margin, which could start in the Eocene, but also could be quite recent. Clade A needs to be further explored as not all species from India have been confidently assigned to this taxonomic group based on morphology (Bouman et al. 2018) and the connection with North America has only recently been confirmed for one species (Bouman et al. 2021). A higher sampling might give a better resolution when these species diverged and spread to different continents.

Our results confirm earlier studies (Kawakita & Kato 2009; Luo et al. 2011b), that tribe Phyllanthae probably diverged from other tribes after the breakup of Gondwana and the breakup of India and Madagascar at 90–85 Ma. The sampling from India in our study is sparse and could represent an interesting aim for future studies. Some species from Sri Lanka (*Cathetus gardnerianus* (Wight) R.W. Bouman and *Nymphanthus floribundus* (Wight) R.W. Bouman), are firmly nested in clades B and C and are found to be of more recent origins in the Miocene

Chapter 9

(Fig. 9-2). The separation of India from Africa and Madagascar is reconstructed to have occurred in the Cretaceous (Ali & Aitchinson 2008; Hall 2012). The much later collision of India with the Asian plate probably occurred somewhere around 35 Ma (Ali & Aitchinson 2008) with a possible earlier connection with Malesia and Myanmar around 57 Ma (Aitchinson et al. 2007). The flora of India harbours species of several clades from tribe Phyllanthae, but not many from those found on Madagascar (see Bouman et al. 2018). The species included here seem to have diverged much more recently and do not support the Indian raft hypothesis for tribe Phyllanthae. However, an expanded sampling of for example the genera *Cathetus* and *Nellica* is necessary to further investigate the relationship of Indian taxa within the tribe.

Out of Africa

Many clades in tribe Phyllanthae contain species distributed in Africa, but unfortunately the major nodes between these groups show less resolution and are usually reconstructed with wide ancestral areas. Dispersals from Africa to other areas can still be inferred in a few clades. *Kirganelia* (Fig. 9-2, node C1) was reconstructed to have an ancestral area in Africa and Asia. *Kirganelia purpurea* (Müll.Arg.) R.W.Bouman and a clade containing several African species is found to be sister to a mixed clade of African, Asian and Malagasy species, which show several dispersal events in the Late Miocene.

Clade D, which consists of three subgenera in *Phyllanthus* in now transferred to the reinstated genus *Moeroris* Raf. (Bouman et al. 2022). This group was estimated to contain almost 200 species (Bouman et al. 2022), which are mostly distributed in Africa. A single dispersal event to Madagascar is found in Clade D during the Miocene and two independent dispersals are found to the Americas. *Moerorist stipulata* Raf. was included here as the only representative of a specific West Indian clade with some species also distributed in South America (see Falcón et al. 2020; Bouman et al. 2021) and it is reconstructed to have diverged from other African species around the Oligocene-Miocene transition. No land bridges are known between these continents at the time when they were much closer to their present day distribution, so this event was likely due to long-distance dispersal. Dispersal from Africa to Madagascar has been inferred to have been easier before a shift in ocean currents around 20–15 Ma (Samonds et al. 2012). Interestingly, the dispersal event within Clade D to Madagascar around the Mid-Miocene (C. 9.8 Ma, HPD 15.76–4.55) occurred either at the end or after this shift. Over-water dispersal could still occur, but was complicated and it is unclear how the species of *Moeroris* crossed this barrier as the capsular fruits are usually not eaten by other dispersal vectors such as birds.

Colonizing the Americas and West Indies

The large Neotropical clade of *Phyllanthus* s.s. (Clade E) seems to have arrived

in South America during the Late Eocene-Oligocene (Fig. 9-2). Following our reconstruction, it diverged from an African ancestor (Fig. 9-2, node 7) at the end of the Eocene. Similar dispersal events were found in other taxa such as platyrrhine monkeys (Seiffert et al. 2020), Arecaceae (Cuenca et al. 2008) and the Clusioid clade of the Malpighiales (Ruhfel et al. 2016), which were attributed also to sea currents (Renner 2003) or a possible boreotropical origin. The majority of Neotropical species of *Phyllanthus*, but also those of the African Clade D, have schizocarpic fruits that self-disperse the seeds. Some observations have been made on how these seeds behave in water (Breteler, pers. comm.), but larger studies on dispersal in *Phyllanthus* have not been done. The ancestral area of Clade E was estimated to be the Neotropics, but *P. purpusii* Brandege, which is sister to the other species of Clade E (Fig. 9-2; Bouman et al. 2021), is from Mexico. This indicates an early dispersal between North and South America at the formation of the Isthmus of Panama (Jaramillo 2018). Other dispersals to North America are difficult to reconstruct here due to sampling limitations as these are from more widespread species. There are some taxa like *P. pseudocicca* Griseb. and *P. subcarnosus* C. Wright ex Griseb. that were proposed to have arrived independently (Falcón et al. 2020), but their phylogenetic position could not be reconstructed with full certainty.

The *Phyllanthus* flora of the West Indies seems to have originated in the Neotropics and it reached the Caribbean at the end of the Oligocene (*P. pachystylus* Urb.) or in the Miocene (majority of *P.* subgenus *Xylophylla*, Fig. 9-2, node E5). To explain the origin of the Caribbean flora, some authors have hypothesized that there was a land-bridge or island chain between South America and the Antilles at the Eocene-Oligocene boundary (Iturralde-Vinent & McPhee 1991). However, this connection was not found for taxa that seemingly originated in South America and dispersed after this period (Nieto-Blázquez et al. 2017). These results seem to be congruent with our findings, that *Phyllanthus* dispersed to the West Indies on several independent occasions, but after the Eocene. A higher sampling of the South American species of *Phyllanthus* could allow for a further scrutiny in dispersal areas between countries as the area is defined here rather wide.

East Malesia, Australia and the New Caledonian interchange

The main diversity of the more than 150 species of *Phyllanthus* subgenus *Gomphidium* is found today on the islands of New Caledonia and Papua New Guinea (Airy Shaw 1980; McPherson & Schmid 1991). The ancestral area of this subgenus is estimated to be Australia with subsequent dispersals to Papua New Guinea and New Caledonia during the Miocene (Fig. 9-2, clade F2). New Caledonia separated from Australia during the Mesozoic and discussions are ongoing whether it and the surrounding islands were completely submerged before the Eocene (Heads 2019). The flora is characterized by high levels of endemism (Pillon et al. 2017), which is also the case with *Dendrophyllanthus* (treated as *P.* subgenus *Gomphidium* in McPherson & Schmid 1991).

Chapter 9

Sister to *Dendrophyllanthus* is clade F1, which corresponds to the genus *Cicca* of which the majority of species occur in Madagascar. Node F was reconstructed as Australia in the Bayarea analysis with low support (Table 9-3), and as Australia & Madagascar by the DEC model around the Mid-Oligocene. This relationship indicates an interesting connection and probable long distance dispersal between Australia and Madagascar (Fig. 9-2). However, it could also be due to incomplete sampling or possible extinction of taxa in areas between these distribution centers, but this cannot be inferred here. Within Clade F1, one group (*Cicca* subgenus *Cicca*) dispersed from Madagascar to Africa around and from there to South America during the Miocene.

Asian spread and diversification

More than 200 species of *Phyllanthus* s.l. occur in Asia and it has been suggested as the area where the genus originated (Govaerts et al. 2000). While this seems unlikely based on our results, Asia still harbours a large diversity of *Phyllanthus* species, which is a mix of several groups. The Asian genus *Nymphanthus* (previously *Phyllanthus* subgenus *Eriococcus*) with a crown age of 23.74 Ma (HPD 31.88–16.28) is reconstructed to have originated on continental Asia, with two independent movements into West Malesia in the Miocene (Fig. 9-2, node C4). Two species of *Nymphanthus* are known from Australia, but only *N. lamprophyllus* (Müll. Arg.) R.W.Bouman is included here and this species also crossed Wallace's line. It diverged from the Australian *Lysiandra* at the Eocene-Oligocene boundary. Another large Asian clade diverged from Node 8 with one group diverging into a clade comprising *Dendrophyllanthus* and the other giving rise to a large Malagasy and African clade.

The origin of the genera *Glochidion* and *Breynia* was inferred to be on the mainland of Asia (Fig. 9-2, node 9). The number of species of the genus *Glochidion* included here is limited and the inclusion of more species could lead to a different interpretation. As inferred here, *Glochidion* is a recently diverged lineage, which has speciated extensively, originating in the Late Miocene (Fig. 9-2). More than 300 species are currently recognized and their radiation has been attributed to a co-diversification with its pollinator (Kato et al. 2003; Kawakita & Kato, 2009). Our reconstruction of *Breynia* is comparable to the results by van Welzen et al. (2015), but their analysis discusses dispersal and vicariance at regional to country levels. The genus *Synostemon* consists of about 40 species and diverged from *Breynia* around 16 Ma (Fig. 9-2, node 11) as the lineage reached Australia and subsequently speciated there.

Diversification of tribe Phyllantheae

Phyllanthus s.l. is composed of several major clades showing distinctly different species numbers, some of which have been inferred to be linked to their specialized pollination system involving a mutualism with parasitic moths (Kato & Kato

2004a). This pollination system and variations of it have been found in several groups of tribe Phyllanthae, most notably in *Glochidion* (Kato et al. 2003), *Breynia* (Kwakita & Kato, 2004b), *Kirganelia* (Kawakita & Kato 2009; Kato & Kawakita 2017), *Dendrophyllanthus* (as *P.* subgenus *Gomphidium*; Kawakita & Kato 2004a) and with some indications for species from Madagascar (Kawakita & Kato 2009; Kato & Kawakita 2017) and the Neotropics (Kawakita et al. 2019). This mutualism has not always resulted in higher species numbers or speciation rates (Fig. 9-3). Speciation rates in *Kirganelia* were similar to *Nymphanthus* and *Cathetus*, for example (Table 9-4), which have been inferred to have different pollination systems (Luo et al. 2011b; Kato & Kawakita 2017). There are about 30 species in the palaeotropical *Kirganelia* (Bouman et al. 2018), which are often widespread and characterized by small pentamerous flowers and berries that are probably dispersed by birds. In contrast, there are more than 150 species in *Dendrophyllanthus* with most of this diversity found in Papua New Guinea and New Caledonia. *Glochidion* contains more than 300 species throughout Southeast Asia. While species in *Dendrophyllanthus* often have capsular fruits, fruits of *Glochidion* also dehisce to present brightly coloured sarcotestal seeds to attract birds. Bird dispersal seems to have resulted in species with wide distributions in *Kirganelia*, possibly constraining speciation rates, but similar patterns are not observed and should be further explored for *Glochidion* and *Dendrophyllanthus*. While the number of studies exploring the finesse and differences of this extraordinary pollination mutualism are steadily increasing, dispersal studies should be included to see how quickly genetic barriers can be raised between populations following isolation.

Conclusion

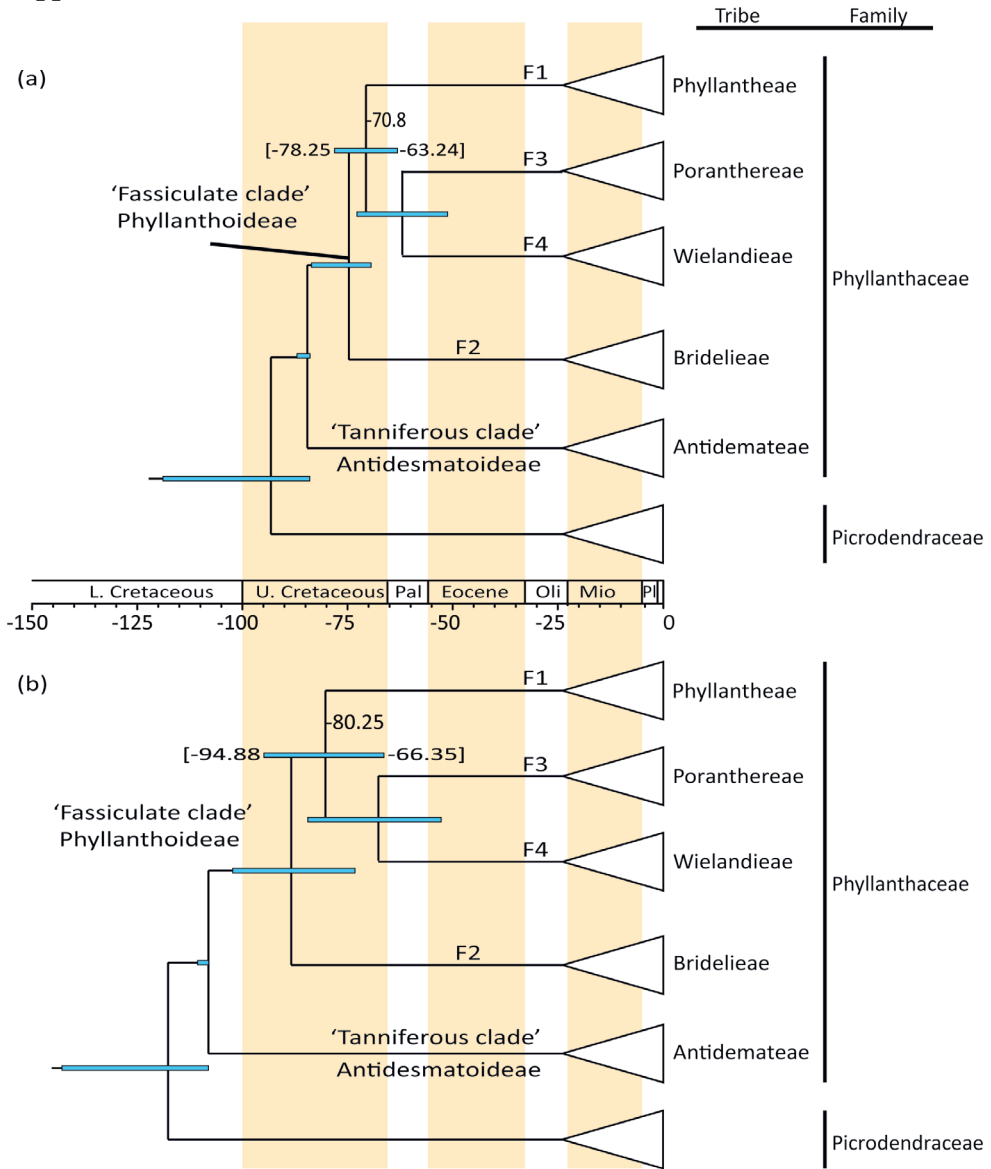
The evolutionary history of tribe Phyllanthae is explored here in more detail. The origin of *Phyllanthus* s.l. is dated to the Early Eocene, congruent with the PETM, while fossil findings in Europe hint at the possibility for a boreotropical origin and or migration pattern. Other theories, such as the Indian Raft hypothesis are unlikely to have played a role in the present distribution of the clade, but enhanced sampling of Indian taxa and taxa associated with *Nellica* (Clade A in Fig. 9-2) should be investigated in future studies to exclude this. Numerous dispersal events in the Cenozoic can be traced to the Miocene geothermal hypothesis or long-distance dispersal. Diversification rates were in general quite low, but a shift detected on node 8 (Fig. 9-2) could be linked to a starting pollination mutualism with moths (Kawakita & Kato 2009), although this was not the only factor as dispersal strategies seem to have constrained further speciation in other clades. Future studies should focus on detailing the various clades of tribe Phyllanthae, where the genera *Flueggea* and *Margaritaria* represent interesting pantropical taxa with bird-dispersed seeds.

Chapter 9

Acknowledgments

This work was done as part of the PhD research of the main author, funded by the Hortus botanicus Leiden (Leiden University) and hosted by Naturalis Biodiversity Center. The second author thanks the Leiden University Fund (LUF) for their support of the chair Botanical gardens and botany of Southeast Asia. The last author thanks the Treub Maatschappij, the Society for the Advancement of Research in the Tropics, for their support of the Ornstein chair in Tropical Plant Biogeography.

Supplement



Supplementary figure S9-1. Summarized chronogram of Phyllanthaceae with tribes collapsed, relevant nodes are shown with 95% HPD; median age of divergence between tribe Phyllanthae and tribe Wielandiae and Poranthereae is given for the different reconstructions above HPD bar. (a) Chronogram of Phyllanthaceae with divergence age with Picrodendraceae constrained at 84 Ma. (b) Chronogram of Phyllanthaceae with divergence age with Picrodendraceae constrained at 108 Ma.

Chapter 9

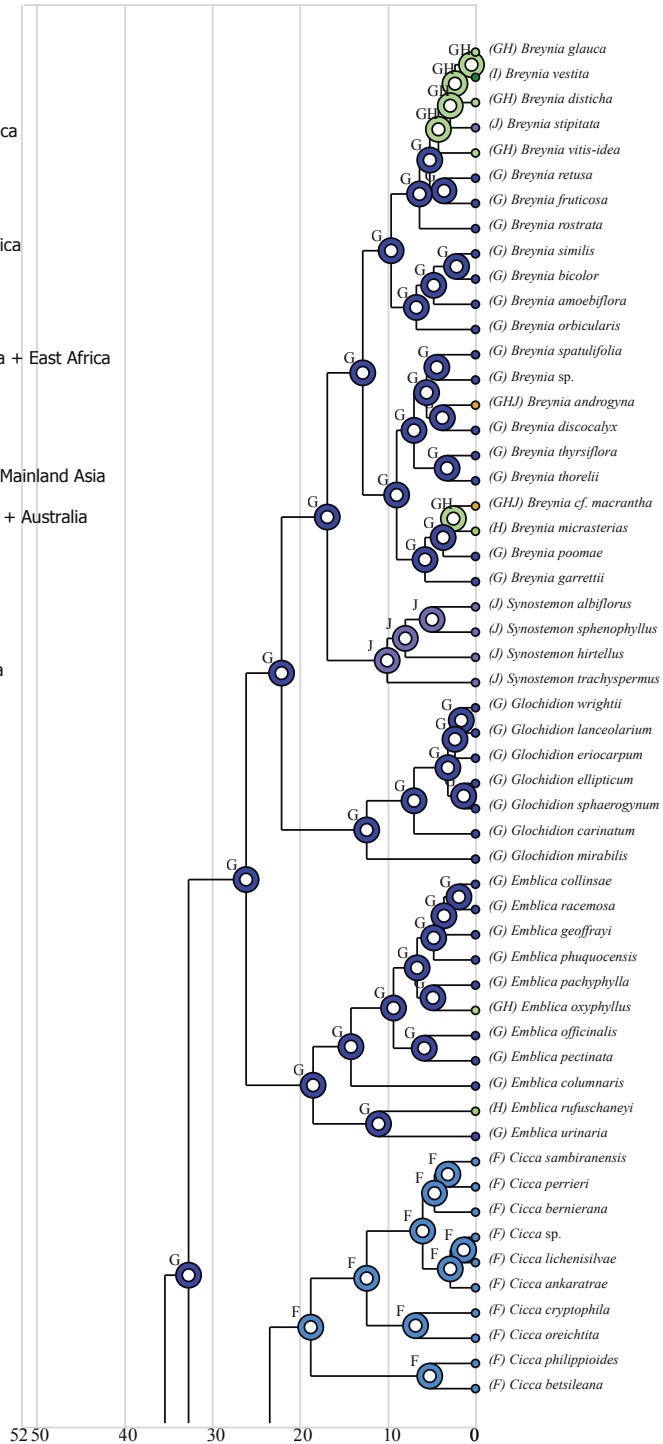
Supplementary figure S9-2. Ancestral area estimations of *Phyllanthus* and ingroup genera following the BAYAREA model. Distributions of taxa are shown at branch tips. Reconstructions on nodes with highest probability are shown. The figure is shown on pages 383 - 386. A full size pdf is available with the author.

Historical biogeography of tribe Phyllantheeae

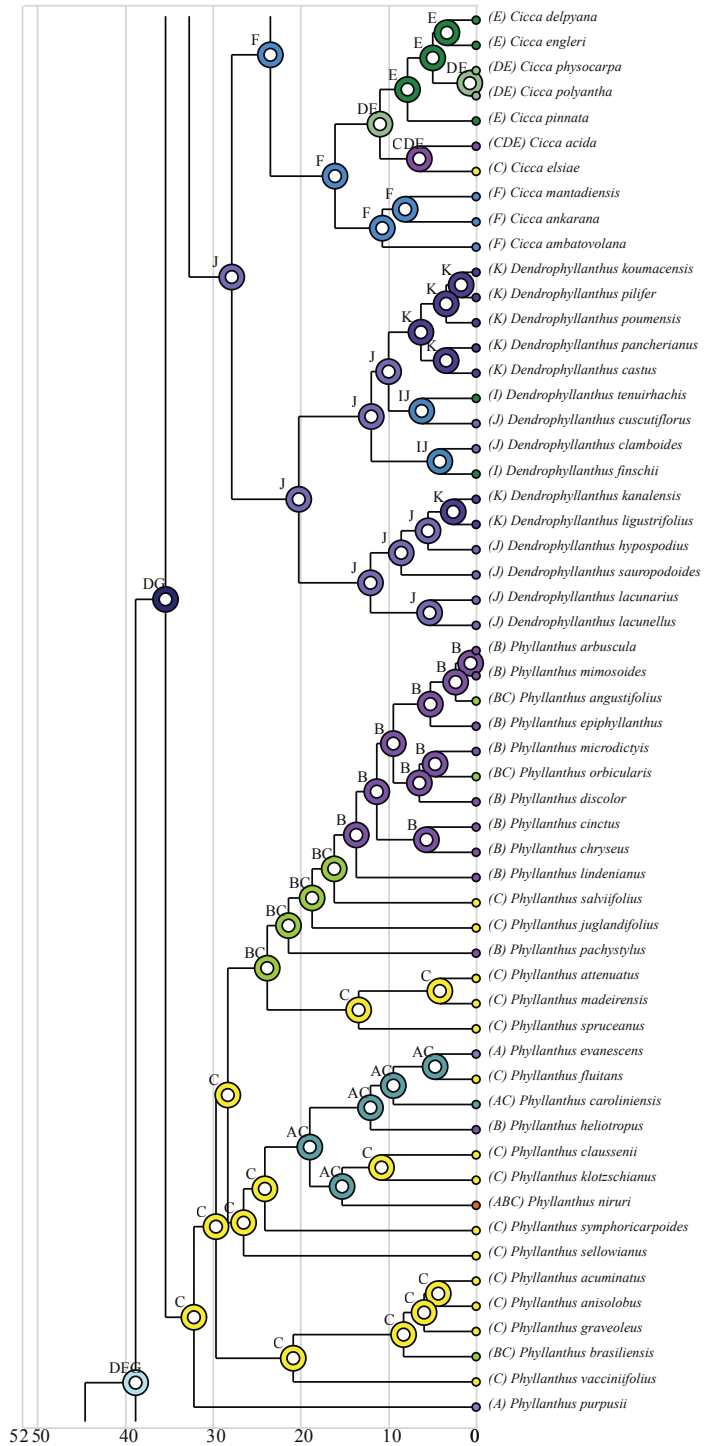
BAYAREALIKE

LEGEND

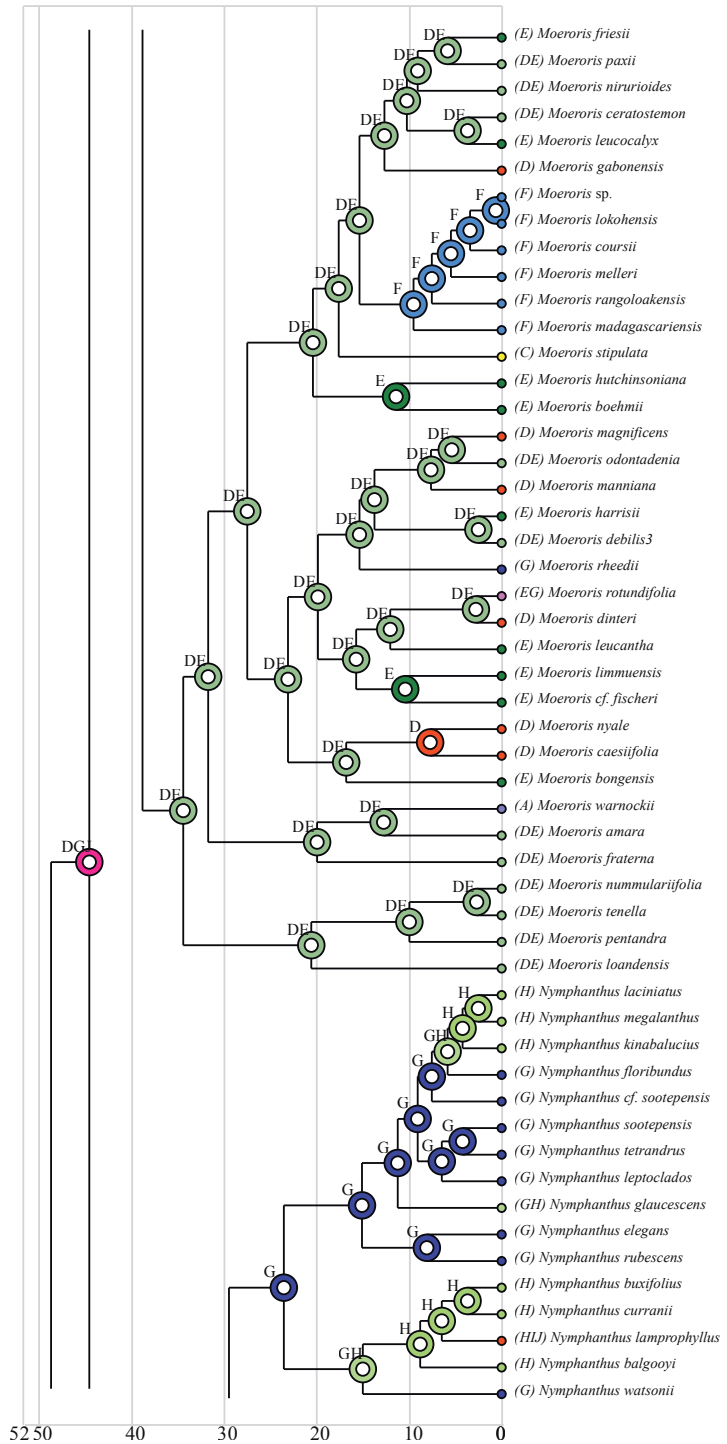
- A North America
- AC North America + South America
- AE North America + East Africa
- B Caribbean Isls.
- BC Caribbean Isls. + South America
- C South America
- CD South America + West Africa
- CDE South America + West Africa + East Africa
- D West Africa
- DE West Africa + East Africa
- DEG West Africa + East Africa + Mainland Asia
- DGJ West Africa + Mainland Asia + Australia
- E East Africa
- F Madagascar
- G Mainland Asia
- GH Mainland Asia + West Malesia
- H West Malesia
- I East Malesia
- IJ West Malesia + East Malesia
- J Australia
- K Pacific



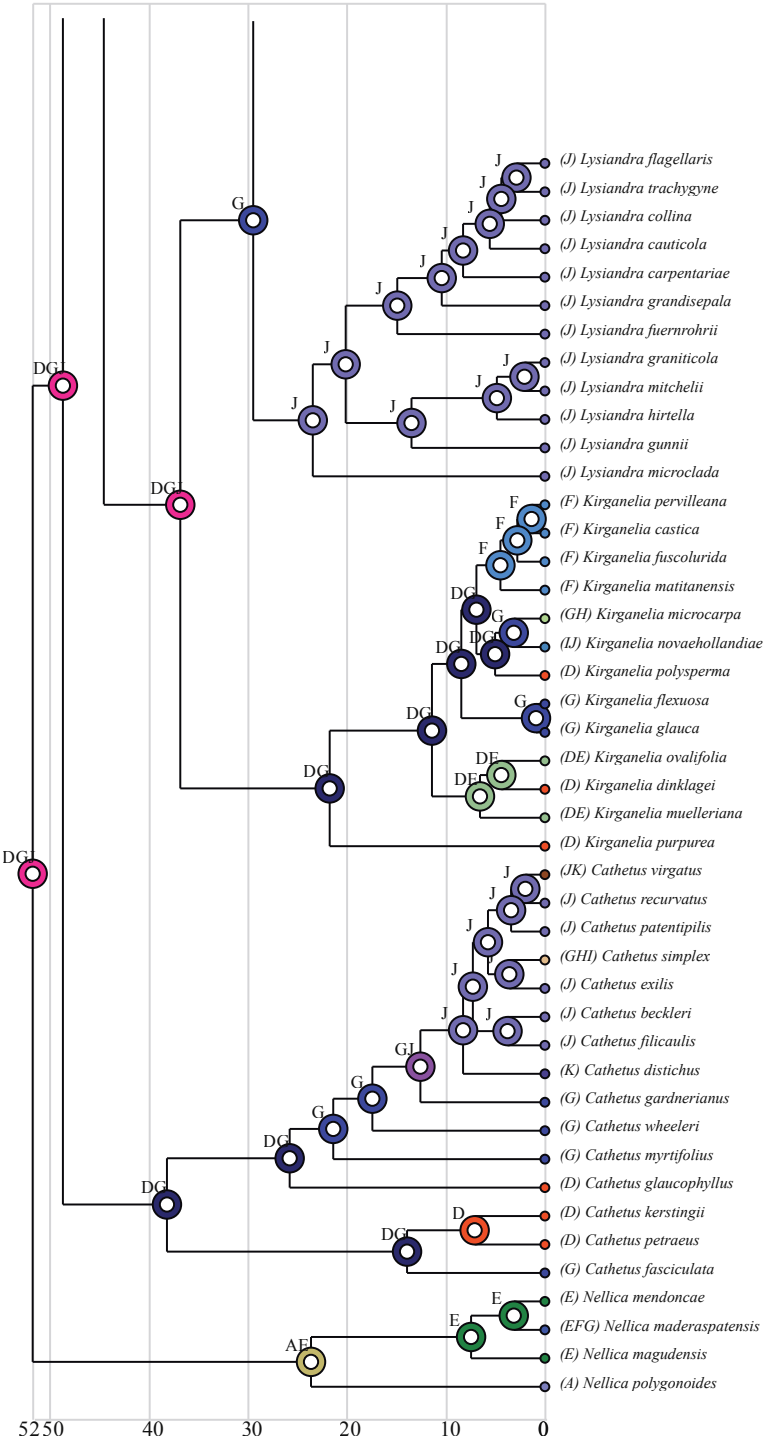
Chapter 9



Historical biogeography of tribe Phyllanthae



Chapter 9



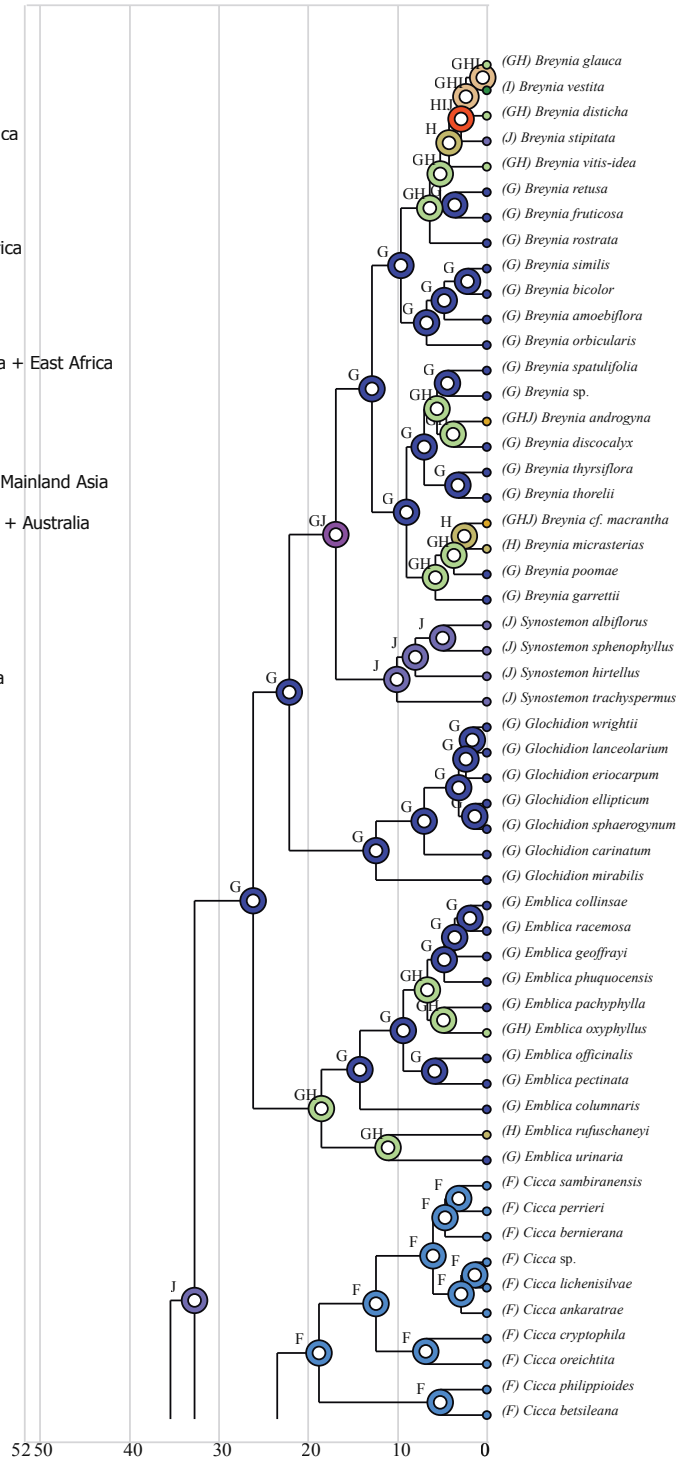
Supplementary figure S9-3. Ancestral area estimations of *Phyllanthus* and ingroup genera following the DEC model. Distributions of taxa are shown at branch tips. Reconstructions on nodes with highest probability are shown. The figure is shown on pages 388 - 391. A full size pdf is available with the author.

Chapter 9

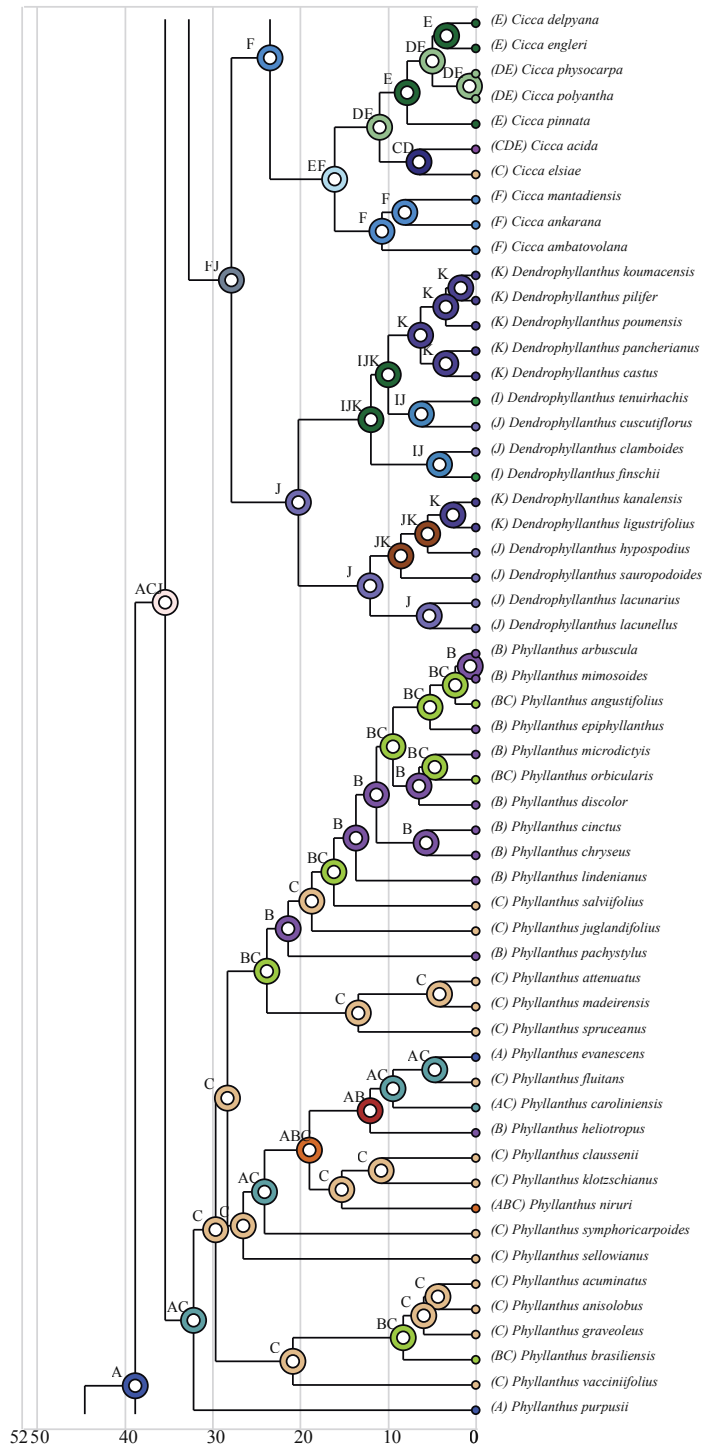
DEC

LEGEND

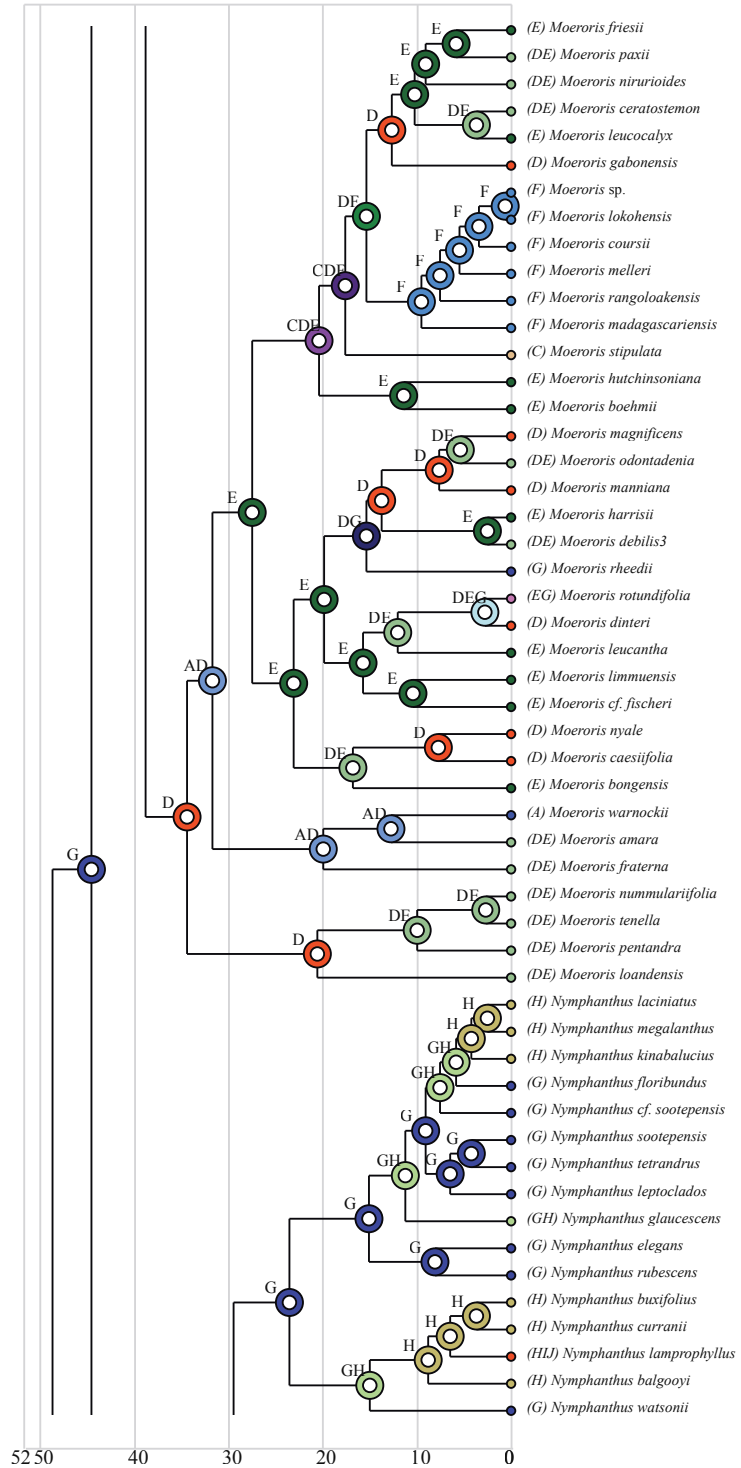
- A North America
- AC North America + South America
- AE North America + East Africa
- B Caribbean Isls.
- BC Caribbean Isls. + South America
- C South America
- CD South America + West Africa
- CDE South America + West Africa + East Africa
- D West Africa
- DE West Africa + East Africa
- DEG West Africa + East Africa + Mainland Asia
- DGJ West Africa + Mainland Asia + Australia
- E East Africa
- F Madagascar
- G Mainland Asia
- GH Mainland Asia + West Malesia
- H West Malesia
- I East Malesia
- IJ West Malesia + East Malesia
- J Australia
- K Pacific



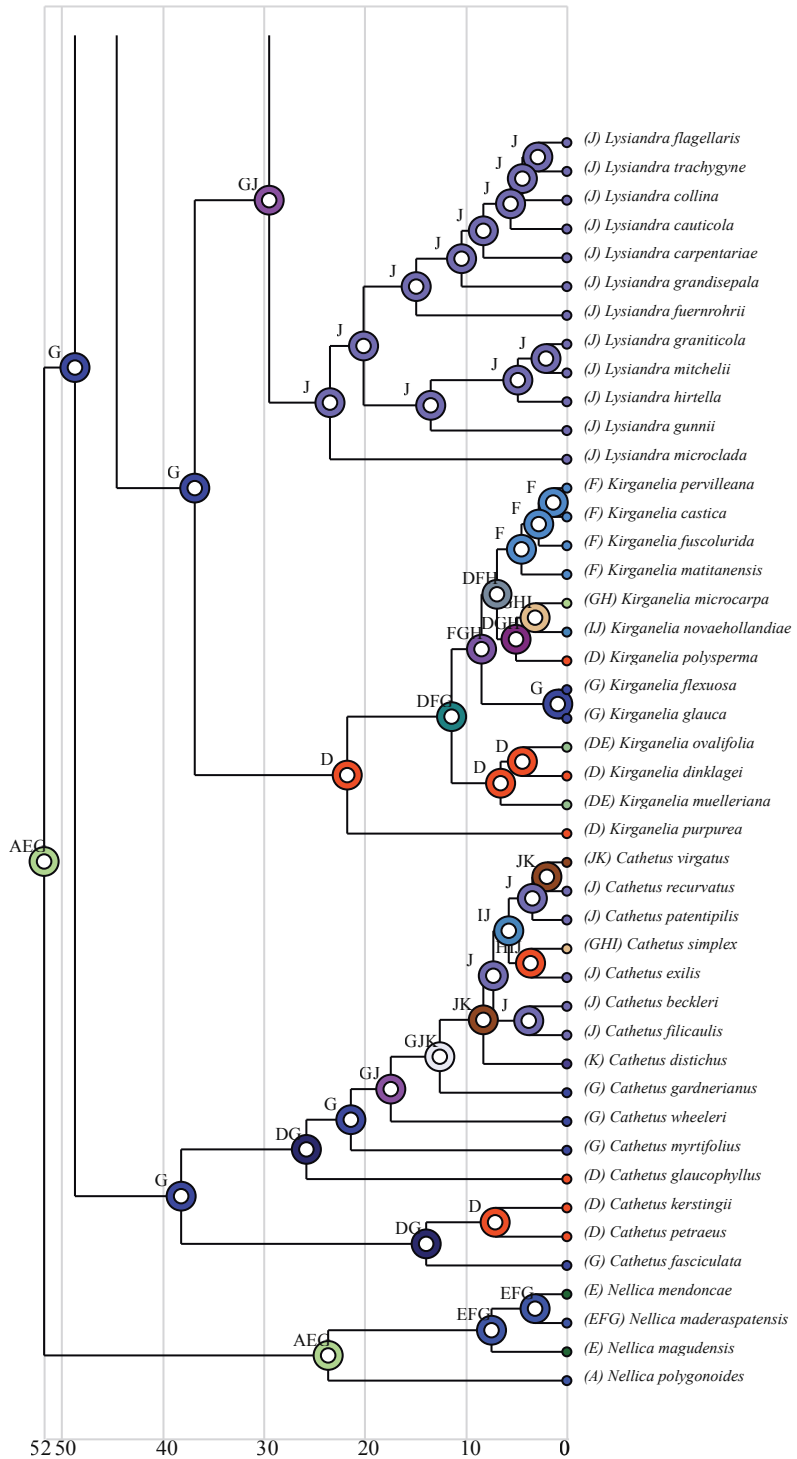
Historical biogeography of tribe Phyllanthae



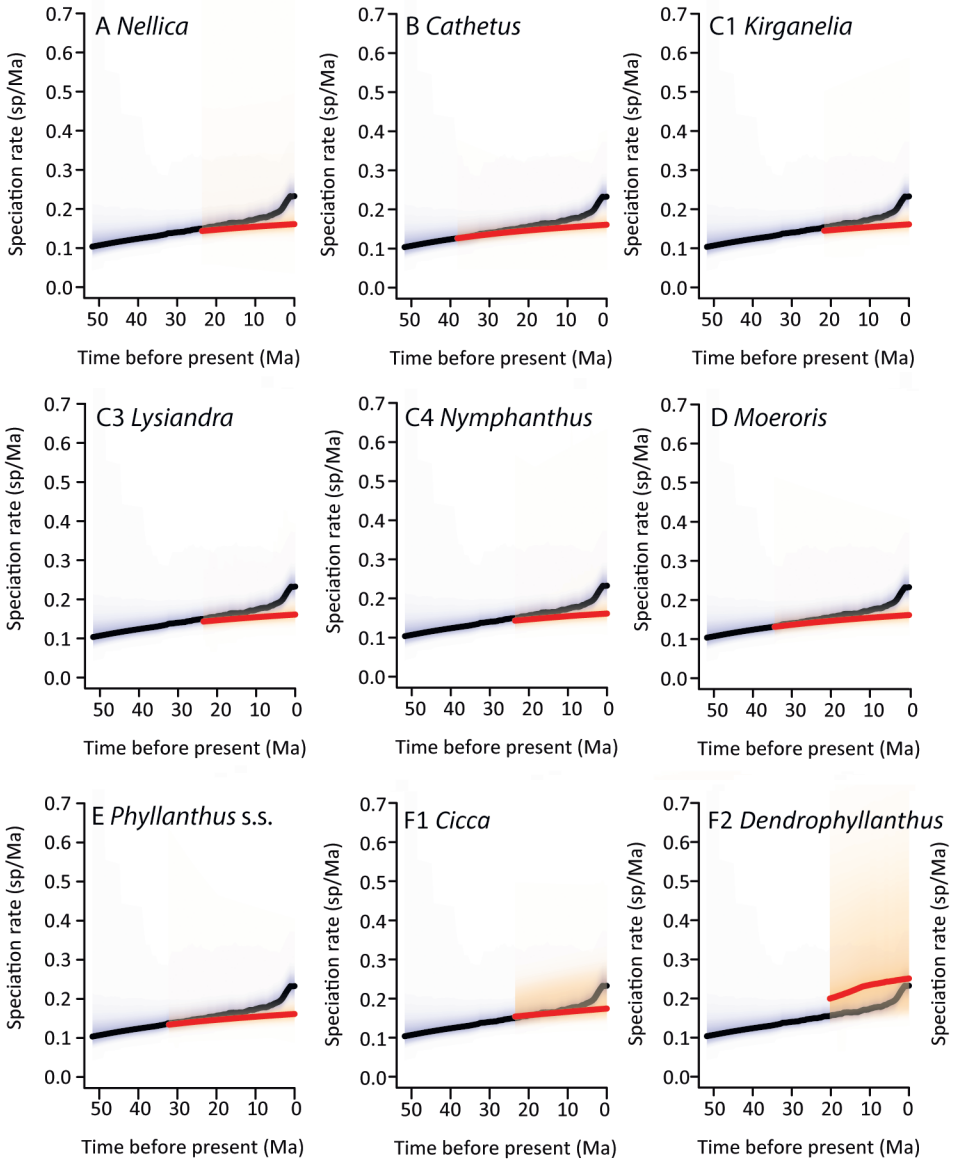
Chapter 9



Historical biogeography of tribe Phyllantheeae

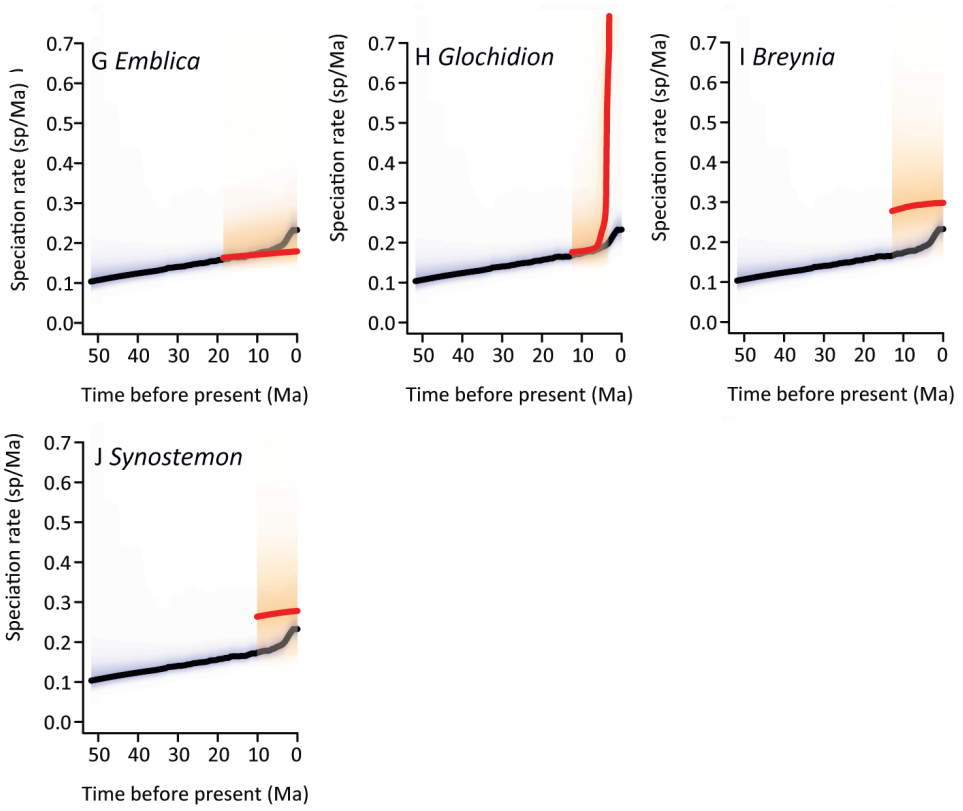


Chapter 9



Supplementary figure S9-4. Additional plots of speciation rates through time of specific clades. Black line represents mean speciation rate through time of the whole phylogeny, red that of a selected clade.

Historical biogeography of tribe Phyllanthae



Supplementary figure S9-4. Continued.

Supplementary table S9-1. Genbank accession numbers of DNA sequences and voucher information for taxa used in this study. Biogeographic regions follow figure 1: A, North America to Mexico; B, West Indies; C, South America and part of the Panama Isthmus; D, West Africa with eastern border following Namibia, Democratic Republic of Congo and Central African Republic; E, South and Eastern Africa; F, Madagascar and the Mascarene Islands; G, W. Asia stretching from India to Peninsular Malaysia; H, W. Malesia including Philippines; I, E. Malesia (mainly Papua New Guinea); J, Australia; K, Islands in the Pacific.

Matrix name	Area code	Origin	ITS	PHYC	accD-psal	matK	trnS-trnG
<i>Breynia amoebiflora</i>	G	Chiang Mai, Thailand				EU643747	
<i>Breynia amoebiflora</i>	G	Thailand	GQ503379	GQ503437	GQ503498		GQ503562
<i>Breynia androgyna</i>	GHJ	Chachoengsao, Thailand	EU623563	GQ503439	GQ503500	EU643748	GQ503564
<i>Breynia bicolor</i>	G	Chiang Mai, Thailand	EU623567		GQ503503	EU643754	
<i>Breynia cfmacrantha</i>	GHJ	China (XTBG)	MN915813	MN904190	MN915297	MN916081	MN915580
<i>Breynia discocalyx</i>	G	Ranong, Thailand	GQ503387			EU643757	GQ503569
<i>Breynia disticha</i>	GH	Singapore botanical garden	MN915815	MN904192	MN915299	MN916083	MN915582
<i>Breynia fruticosa</i>	G	Hong Kong	MN915816	MN904193	MN915300	MN916084	MN915583
<i>Breynia garrettii</i>	G	Guizhou, China	EU623570	GQ503444	GQ503507	EU643760	GQ503572
<i>Breynia glauca</i>	GH	Nong Khai, Thailand	EU623551	GQ503411		EU643737	GQ503532
<i>Breynia micrasterias</i>	H	Sarawak, Malaysia	EU623578	GQ503455		EU643768	GQ503582
<i>Breynia orbicularis</i>	G	Vientiane, Laos	EU623580	GQ503456	GQ503513	AY936645	GQ503584
<i>Breynia poomae</i>	G	Chiang Rai, Thailand	EU623582	GQ503457	GQ503515	EU643771	GQ503586
<i>Breynia retusa</i>	G	Sri Lanka				AY936565	
<i>Breynia retusa</i>	G	Vientiane, Laos	GQ503358	GQ503417	GQ503477		GQ503536
<i>Breynia rostrata</i>	G	China (XTBG)	MN915817	MN904194	MN915301	MN916086	MN915585

<i>Breynia similis</i>	G	Chiang Mai, Thailand	GQ503399	GQ503462	GQ503520	EU643778	GQ503592
<i>Breynia</i> sp.	G	Thailand	MN915843	MN904215	MN915327	MN916112	MN915600
<i>Breynia spatulifolia</i>	G	Honolulu, U.S.A.	EU623588		GQ503523	AY936647	GQ503596
<i>Breynia stipitata</i>	J	RBG Kew, Living collection from Queensland, Australia				AY552422	
<i>Breynia stipitata</i>	G	Australia	GQ503359	GQ503418	GQ503478		GQ503537
<i>Breynia thorelii</i>	G	Chiang Mai, Thailand	EU623590	GQ503468	GQ503526	EU643782	GQ503600
<i>Breynia thyrsoiflora</i>	G	Kanchanaburi, Thailand	EU623591	GQ503469	GQ503527	EU643783	GQ503601
<i>Breynia vestita</i>	I	Papua, Indonesia	EU623553	GQ503419	GQ503480	EU643738	GQ503540
<i>Breynia vitis-idea</i>	GH	Singapore botanical garden	MN915822	MN904187	MN915306	MN916090	MN915587
<i>Cathetus beckleri</i>	J	Australia	MN915861	MN904231	MN915347	MN916127	MN915618
<i>Cathetus distichus</i>	K	Hawai'i	MN915912	MN904276	MN915404	MN916163	MN915665
<i>Cathetus exilis</i>	J	Australia	MN915922	MN904283		MN916362	MN915672
<i>Cathetus fasciculata</i>	G	Hong Kong	MN915895	MN904262	MN915384	MN916154	MN915648
<i>Cathetus filicaulis</i>	J	Australia	MN915923	MN904284	MN915415	MN916170	MN915673
<i>Cathetus gardnerianus</i>	G	Sri Lanka	AY936694	MN904314	MN915429	AY936598	MN915684
<i>Cathetus glaucophyllus</i>	DE	Guinea	MN915939	MN904318	MN915433	MN916340	MN915688
<i>Cathetus kerstingii</i>	D	Guinea	MN915950	MN905074	MN915447	MN916189	MN915701
<i>Cathetus myrtifolius</i>	G	Hong Kong University campus	MN915995	MN904370	MN915495	MN916214	MN915736
<i>Cathetus patentipilis</i>	J	Australia	MN916020	MN904392	MN915518	MN916234	MN915759
<i>Cathetus petraeus</i>	D	Liberia	MN916026	MN904397	MN915524	MN916239	MN915763
<i>Cathetus recurvatus</i>	J	Australia	MN916046	MN904414	MN915543	MN916258	MN915778

Chapter 9

<i>Cathetus simplex</i>	G	Hong Kong	MN916074	MN904440	MN915572	MN916276	MN915805
<i>Cathetus virgatus</i>	J	Australia	AY936738	MN904442	MN915574	AY936639	MN915807
<i>Cathetus wheeleri</i>	G	Sri Lanka	AY936740	MN904445	MN915577	AY936641	MN915810
<i>Cicca acida</i>	CDE	Thailand	MN915836	GQ503432	GQ503492	MN916108	GQ503556
<i>Cicca ambatovolana</i>	F	Madagascar	MN915848	MN904218	MN915332	MN916115	MN915605
<i>Cicca ankarana</i>	F	Madagascar	MN915851	MN904221	MN915335	MN916118	MN915608
<i>Cicca ankaratrae</i>	F	Madagascar	MN915852	MN904222	MN915336	MN916119	MN915609
<i>Cicca bernierana</i>	F	Madagascar	MN915862	MN904232	MN915348	MN916128	MN915619
<i>Cicca betsileana</i>	F	Madagascar	MN915863	MN904233	MN915349	MN916360	MN915620
<i>Cicca cryptophila</i>	F	Madagascar	MN915899	MN904265	MN915390	MN916358	MN915653
<i>Cicca delpyana</i>	DE	Republic of the Congo	MN915906		MN915397	MN916161	MN915659
<i>Cicca elisiae</i>	C	Venezuela	MN915916	MN904278	MN915408	MN916337	MN915667
<i>Cicca engleri</i>	E	Tanzania		MN905066	MN915410	MN916168	MN915669
<i>Cicca lichenisilvae</i>	F	Madagascar		MN904343	MN915464	MN916199	
<i>Cicca mantadiensis</i>	F	Madagascar	MN915980	MN904354	MN915480	MN916319	
<i>Cicca oreichtita</i>	F	Madagascar	MN916013	MN904385		MN916226	
<i>Cicca perrieri</i>	F	Madagascar	MN916024	MN904395	MN915522	MN916238	MN915762
<i>Cicca philippioides</i>	F	Madagascar	MN916027	MN904398	MN915525	MN916240	MN915764
<i>Cicca physocarpa</i>	DE	Gabon	MN916030	MN904401	MN915528	MN916243	MN915766
<i>Cicca pinnata</i>	E	Zimbabwe	MN916032	MN904403	MN915530	MN916245	MN915704
<i>Cicca polyantha</i>	DE	Cameroon	MN916033		MN915531	MN916246	MN915767
<i>Cicca sambiranensis</i>	F	Madagascar	MN916053	MN904421	MN915552	MN916315	MN915784
<i>Cicca sp.</i>	F	Madagascar	MN915845	MN904295	MN915329	MN916282	
<i>Dendrophyllanthus castus</i>	K	New caledonia	MN915879	MN904246	MN915367	MN916327	MN915632

<i>Dendrophyllanthus clamboides</i>	J	Australia	MN915893	MN904260	MN915382	MN916152	MN915646
<i>Dendrophyllanthus cuscutiflorus</i>	IJ	Singapore botanical garden origin East Malasia	MN915901	MN904268	MN915392	MN916299	MN915654
<i>Dendrophyllanthus finschii</i>	I	Papua New Guinea	MN915924	MN904285	MN915416	MN916171	MN915674
<i>Dendrophyllanthus hypospodius</i>	J	Australia		GQ503435	GQ503495	EU643744	GQ503559
<i>Dendrophyllanthus kanalensis</i>	K	New Caledonia	AY936701			AY936604	
<i>Dendrophyllanthus koumacensis</i>	K	New Caledonia	MN915953	MN904331	MN915451	MN916191	
<i>Dendrophyllanthus lacunarius</i>	J	Australia	MN915955	MN904333	MN915453	MN916312	MN915706
<i>Dendrophyllanthus lacunellus</i>	J	Australia	MN915956	MN904334	MN915454	MN916313	MN915707
<i>Dendrophyllanthus ligustrifolius</i>	K	New Caledonia	MN915966	MN904309	MN915466	MN916311	MN915714
<i>Dendrophyllanthus pancherianus</i>	K	New Caledonia	AY936721	MN904391	MN915517	AY936623	MN915758
<i>Dendrophyllanthus pilifer</i>	K	New Caledonia	MN916031	MN904402	MN915529	MN916244	
<i>Dendrophyllanthus poumensis</i>	K	New Caledonia	MN916039	MN904408	MN915537	MN916251	MN915772
<i>Dendrophyllanthus sauropodoides</i>	J	Australia	EU623558	GQ503436	GQ503496	EU643745	GQ503560

Chapter 9

<i>Dendrophyllanthus tenuirhachis</i>	I	Bogor botanical garden	MN916068	MN904435	MN915567	MN916271	MN915800
<i>Emblcia oxyphylla</i>	G	Thailand	MN916018	MN904388	MN915515	MN916232	MN915755
<i>Emblcia pectinata</i>	G	Singapore botanical garden origin Mainland Asia	MN916022		MN915520	MN916236	MN915761
<i>Emblcia phuquocensis</i>	G	Cambodia	MN916029	MN904400	MN915527	MN916242	
<i>Emblcia racemosa</i>	G	Sri Lanka	MN916035	MN904405	MN915533	MN916248	MN915769
<i>Emblcia collinsae</i>	G	Thailand	MN915896	MN904263	MN915385	MN916155	MN915649
<i>Emblcia columnaris</i>	G	Myanmar		MN904302	MN915387	MN916157	MN915651
<i>Emblcia geoffrayi</i>	G	Thailand	MN915936	MN904315	MN915430	MN935816	MN915685
<i>Emblcia officinalis</i>	G	Myanmar	MN915917	MN904279	MN915409	MN916167	MN915668
<i>Emblcia pachyphylla</i>	G	Viet Nam	MN915853	MN904223	MN915337	MN916120	
<i>Emblcia rufuschaneyi</i>	H	Borneo		MN904418	MN915547	MN916259	MN915781
<i>Emblcia urinaria</i>	G	Hortus botanicus Leiden, origin Costa rica	MN916072	MN904438	MN915570	MN916274	MN915803
<i>Flueggea virosa</i>		China (XTBG)	MN915824	MN904197	MN915308	MN916091	
<i>Glochidion carinatum</i>	G	Cambodia		MN904243	MN915363	MN916138	
<i>Glochidion ellipticum</i>	G	China (XTBG)	MN915827	MN904200	MN915311	MN916094	MN915590
<i>Glochidion eriocarpum</i>	G	Hong Kong	MN915828	MN904201		MN916095	MN915592
<i>Glochidion lanceolarium</i>	G	China (XTBG)	MN915830	MN904203	MN915312	MN916097	MN915593
<i>Glochidion mirabilis</i>	G	Thailand	HM132100	HM132101	HM132099		HM132102
<i>Glochidion sphaerogynum</i>	G	Thailand	MN915831	MN904204	MN915313	MN916280	MN915594

<i>Glochidion wrightii</i>	G	Hong Kong	MN915832	MN904205	MN915314	MN916098	MN915595
<i>Kirganelia castica</i>	F	Madagascar	MN915878	MN904244	MN915366	MN916141	
<i>Kirganelia dinklagei</i>	E	Gabon	MN915908	MN904273	MN915399	MN916333	MN915660
<i>Kirganelia flexuosa</i>	GH	Myanmar	MN915929	MN904288	MN915421	MN916172	MN915679
<i>Kirganelia fuscolurida</i>	F	Madagascar	MN915934	MN904296	MN915426	MN916179	
<i>Kirganelia glauca</i>	G	Hong Kong	MN915940	MN904291	MN915434	MN916175	MN915689
<i>Kirganelia matitanensis</i>	F	Madagascar	MN915981	MN904355	MN915481	MN916205	
<i>Kirganelia microcarpa</i>	G	China (XTBG)	MN915985	MN904358	MN915483	MN916207	MN915729
<i>Kirganelia muelleriana</i>	DE	Zambia	MN915992	MN904368	MN915492	MN916212	MN915734
<i>Kirganelia novae-hollandiae</i>	J	Australia	MN916001	MN904376	MN915500	MN916219	MN915741
<i>Kirganelia pervilleana</i>	F	Madagascar	MN916025	MN904396	MN915523	MN916351	
<i>Kirganelia polysperma</i>	DE	Ethiopia	MN916036	MN904386	MN915534	MN916230	MN915771
<i>Kirganelia purpurea</i>	E	Namibia	MN916042	MN904411	MN915540	MN916254	MN915775
<i>Leptopus chinensis</i>		Cultivated Edinburgh Botanical garden	MN915833	MN904206	MN915315	MN916099	
<i>Lysiandra carpentariae</i>	J	Australia	MN915877	MN905063	MN915365	MN916140	MN915631
<i>Lysiandra caucicola</i>	J	Australia	MN915881	MN904247	MN915369	MN916303	MN915633
<i>Lysiandra collina</i>	J	Australia		MN904264	MN915386	MN916156	MN915650
<i>Lysiandra fuernrohrii</i>	J	Australia		MN904294		MN916178	
<i>Lysiandra grandisepalus</i>	J	Australia	MN915942	MN904319	MN915436	MN916289	MN915690
<i>Lysiandra graniticola</i>	J	Australia	MN915943	MN904320	MN915437	MN916185	MN915691
<i>Lysiandra gunnii</i>	J	Australia	MN915944	MN904322	MN915439	MN916290	MN915693
<i>Lysiandra hirtella</i>	J	Australia	MN915947	MN904326	MN915442	MN916187	MN915697

<i>Lysiandra microclada</i>	J	Australia	MN915988	MN904362	MN915487	MN916320	MN915730
<i>lysiandra mitchellii</i>	J	Australia	MN915990	MN904365	MN915490	MN916210	MN915733
<i>Lysiandra trachygyne</i>	J	Australia	MN916069	MN904436	MN915568	MN916294	MN915801
<i>Margaritaria discoidea</i>		Kenya		MN904207	MN915316	MN916101	
<i>Margaritaria indica</i>		Singapore botanical garden		MN904209	MN915318	MN916105	
<i>Margaritaria nobilis</i>		Puerto Rico		MN904210	MN915319	MN916106	MN915596
<i>Margaritaria Uganda</i>		Uganda	MN915835	MN904211	MN915320	MN916107	MN915597
<i>Moeroris amara</i>	DE	Thailand	EU623557	GQ503433	GQ503493	EU643742	GQ503557
<i>Moeroris arenaria</i>	A	USA (Texas)	AY936743	AY830380		AY830280	
<i>Moeroris boehmii</i>	E	Kenya	MN915865	MN904234	MN915351	MN916129	MN915622
<i>Moeroris bongensis</i>	E	Ethiopia	MN915868	MN904305	MN915355	MN916284	
<i>Moeroris caesifolius</i>	D	Cameroon	MN915875	MN904242	MN915362	MN916137	MN915629
<i>Moeroris ceratostemon</i>	E	Tanzania	MN915882	MN904248	MN915370	MN916142	MN915634
<i>Moeroris cf.fischeri</i>	E	Ethiopia	MN915887	MN905067	MN915375	MN916343	MN915725
<i>Moeroris coursii</i>	F	Madagascar	MN915898	MN904266	MN915389	MN916329	
<i>Moeroris debilis</i>	DE	Philippines	MN915905	MN904271	MN915396	MN916332	MN915658
<i>Moeroris dinteri</i>	E	Namibia	MN915911	MN905069	MN915402	MN916336	MN915663
<i>Moeroris flagellaris</i>	J	Australia	MN915926	MN904287	MN915418	MN916307	MN915676
<i>Moeroris fraternus</i>	AE	Pakistan	MN915931		MN915423	MN916306	MN915681
<i>Moeroris friesii</i>	E	Zambia	MN915932	MN904293	MN915424	MN916177	MN915682
<i>Moeroris gabonensis</i>	D	Gabon	MN915935	MN904313	MN915428	MN916182	
<i>Moeroris harrisii</i>	E	Tanzania	MN915945	MN904323	MN915440	MN916341	MN915694
<i>Moeroris hutchinsoniana</i>	E	Zimbabwe	AY936697	MN904327	MN915443	AY936660	MN915698

<i>Moeroris leucantha</i>	E	Ethiopia	MN915963	MN904340	MN915461	MN916344	MN915713
<i>Moeroris leucocalyx</i>	E	Tanzania	MN915964	MN904342	MN915463	MN916198	
<i>Moeroris limmuensis</i>	E	Ethiopia	MN915967	MN904345	MN915467	MN916291	MN915715
<i>Moeroris loandensis</i>	E	Malawi	MN915968	MN904346	MN915469	MN916201	MN915717
<i>Moeroris lokohensis</i>	F	Madagascar	MN915971	MN904347		MN916316	
<i>Moeroris madagascariensis</i>	F	Madagascar	MN915973	MN904348	MN915473	MN916317	
<i>Moeroris magnificens</i>	D	Guinea	MN915975	MN904349	MN915475	MN916345	MN915722
<i>Moeroris manniana</i>	E	Cameroon	MN915977	MN904351	MN915477	MN916347	MN915724
<i>Moeroris melleri</i>	F	Madagascar	MN915983	MN904357	MN915482	MN916314	MN915728
<i>Moeroris nirurtoides</i>	DE	Gabon	MN915999	MN904375	MN915498	MN916218	MN915740
<i>Moeroris nummulariifolia</i>	DEF	Tanzania	MN916005	MN904379	MN915504	MN916222	
<i>Moeroris nyale</i>	D	Cameroon	MN916008	MN904382	MN915507	MN916224	MN915746
<i>Moeroris odontadenia</i>	DE	Utrecht botanical garden	MN916010	MN904383	MN915509	MN916349	MN915748
<i>Moeroris ovalifolia</i>	DE	Ethiopia	MN916016	MN904301	MN915514	MN916229	MN915753
<i>Moeroris paxii</i>	E	Tanzania	MN916021	MN904393	MN915519	MN916235	MN915760
<i>Moeroris pentandrus</i>	E	Malawi	MN916023	MN904394	MN915521	MN916237	
<i>Moeroris rangoloakensis</i>	F	Madagascar	MN916045	MN904413	MN915542	MN916257	MN915777
<i>Moeroris rheedii</i>	G	Sri Lanka	AY936729	MN904415	MN915544	AY936630	MN915779
<i>Moeroris rotundifolius</i>	E	Kenya	MN916047	MN904416	MN915545	MN916352	MN915780
<i>Moeroris sp.</i>	F	Madagascar	MN915846		MN915330	MN916281	
<i>Moeroris stipulata</i>	C	Suriname	MN916062	MN904431	MN915562	MN916269	MN915794

Chapter 9

<i>Moeroris tenella</i>	J	Australia	MN916065	MN904433	MN915564	MN916354	MN915797
<i>Nellica maderaspatensis</i>	F	Madagascar	AY936707			AY936609	
<i>Nellica magudensis</i>	DE	Sudan	MN915976	MN904350	MN915476	MN916318	MN915723
<i>Nellica mendoncae</i>	E	Ethiopia	MN915984				
<i>Nellica polygonoides</i>	A	USA (Texas)	MN916034	MN904404	MN915532	MN916247	MN915768
<i>Notoleptopus decaisnei</i>		Australia	AM745836			AM745833	
<i>Notoleptopus decaisnei</i>		Australia		GQ503431	GQ503491		GQ503555
<i>Nymphanthus aff. curranii</i>	H	Philippines	MN915900	MN904267	MN915391	MN916158	MN915604
<i>Nymphanthus balgooyi</i>	H	Philippines	MN915860	MN904230	MN915346	MN916325	MN915617
<i>Nymphanthus buxifolius</i>	H	Singapore botanical garden	MN915873	MN904240	MN915360	MN916326	MN915627
<i>Nymphanthus elegans</i>	G	Viet Nam	MN915915	MN904277	MN915407	MN916166	
<i>Nymphanthus floribundus</i>	G	Sri Lanka	AY936682	MN904259	MN915381	AY936587	
<i>Nymphanthus glaucescens</i>	G	Thailand	MN916041	MN904410	MN915539	MN916253	MN915774
<i>Nymphanthus kinabalucius</i>	H	Borneo	MN915952	MN904330	MN915449	MN916190	MN915703
<i>Nymphanthus laciniatus</i>	H	Philippines	MN915954	MN904332	MN915452	MN916192	MN915705
<i>Nymphanthus lamprophyllus</i>	J	Australia	MN915959	MN904337	MN915457	MN916195	MN915710
<i>Nymphanthus leptoclados</i>	G	China (XTBG)	MN915961	MN904339	MN915459	MN916196	MN915712

Historical biogeography of tribe Phyllanthae

<i>Nymphanthus megalanthus</i>	H	Philippines	MN915982	MN904356		MN916206	MN915727
<i>Nymphanthus rubescens</i>	G	Viet Nam	MN916048	MN904417	MN915546	MN916322	
<i>Nymphanthus sootepensis</i>	G	Myanmar	MN916059	MN904426	MN915558	MN916297	MN915790
<i>Nymphanthus tetrandrus</i>	G	Myanmar	MN916058	MN904425	MN915557	MN916296	MN915789
<i>Nymphanthus watsonii</i>	G	Peninsular Malaysia	MN916076	MN904444	MN915576	MN916278	MN915809
<i>Phyllanthus acuminatus</i>	C	Guatemala	MN915838	MN904213	MN915322	MN916110	MN915599
<i>Phyllanthus angustifolius</i>	B	Bayreuth botanical garden living collection origin Carribean	MN915849	MN904219	MN915333	MN916116	MN915606
<i>Phyllanthus anisolobus</i>	C	Costa Rica	MN915850	MN904220	MN915334	MN916117	MN915607
<i>Phyllanthus arbuscula</i>	B	Meisse living collection origin Carribean	MN915855	MN904226	MN915339	MN916123	MN915610
<i>Phyllanthus attenuatus</i>	C	Venezuela	MN915856	MN904304	MN915341	MN916125	MN915612
<i>Phyllanthus brasiliensis</i>	C	Peru, Loreto, Pongo de Cainarachi	MN915871	MN904236	MN915358	MN916135	MN915626
<i>Phyllanthus caroliniensis</i>	ABC	Suriname	MN915876		MN915364	MN916139	MN915630
<i>Phyllanthus cf. sootepensis</i>	G	China (XTBG)	MN915890	MN904428	MN915378	MN916267	MN915643
<i>Phyllanthus chryseus</i>	B	Cuba	AY936681	MN904257	MN915379	AY936586	MN915644
<i>Phyllanthus cinctus</i>	B	Cuba	MN915892	MN904258	MN915380	MN916151	MN915645

Chapter 9

<i>Phyllanthus clausenii</i>	C	Minas Gerais	MN915894	MN904261	MN915383	MN916153	MN915647
<i>Phyllanthus discolor</i>	B	Cuba	AY936688	MN904275	MN915403	AY936593	MN915664
<i>Phyllanthus epiphyllanthus</i>	B	Meisse living collection	MN915919	MN904280	MN915412	MN916169	MN915671
<i>Phyllanthus evanescens</i>	AC	Nicaragua	MN915921	MN904282	MN915414	MN916339	
<i>Phyllanthus fluitans</i>	C	Cultivated Botanical garden Bonn	MN915930	MN904292	MN915422	MN916176	MN915680
<i>Phyllanthus graveolens</i>	C	Ecuador	AY936696	MN904321	MN915438	AY936600	MN915692
<i>Phyllanthus heliotropus</i>	B	Cuba	MN915946	MN904325	MN915441	MN916186	MN915696
<i>Phyllanthus juglandifolius</i>	C	Cultivated, Hortus botanicus Amsterdam origin South America	MN915949	MN904328	MN915445	MN916188	MN915699
<i>Phyllanthus klotzschianus</i>	C	Brazil	AY936702			AY936605	
<i>Phyllanthus lindianus</i>	B	Dominican Republic	LS975755			LS975815	
<i>Phyllanthus lindianus</i>	B	Dominican Rep.			MN915468		MN915716
<i>Phyllanthus madeirensis</i>	C	Brazil	MN915974	MN905078	MN915474	MN916293	MN915721
<i>Phyllanthus microdictyis</i>	B	Cuba	AY936709	MN904363	MN915488	AY936612	MN915731
<i>Phyllanthus mimosoides</i>	B	Meisse living collection origin Carribean	MN915989	MN904364	MN915489	MN916209	MN915732
<i>Phyllanthus niruri</i>	C	Bolivia	MN916000	MN904373	MN915499	MN916217	
<i>Phyllanthus orbicularis</i>	B	Cuba	MN916012	MN904298	MN915511	MN916225	MN915750

Historical biogeography of tribe Phyllantheae

<i>Phyllanthus pachystylus</i>	B	Cuba	AY936720	MN904390	MN915516	AY936622	MN915757
<i>Phyllanthus purpusii</i>	A	Mexico, now cultivated Berkeley	MN916043	MN904412	MN915541	MN916255	MN915776
<i>Phyllanthus salviifolius</i>	C	Ecuador	MN916052	MN904420	MN915551	MN916262	MN915783
<i>Phyllanthus sellowianus</i>	C	Kew living collection	MN916056	MN904424	MN915555	MN916265	MN915787
<i>Phyllanthus spruceanus</i>	C	Guyana	MN916061	MN904429	MN915560	MN916353	MN915792
<i>Phyllanthus symphoricarpoides</i>	C	Colombia	MN916064	MN904307	MN915563	MN916321	MN915796
<i>Phyllanthus vacciniifolius</i>	C	Venezuela	MN916073	MN904439	MN915571	MN916275	MN915804
<i>Synostemon albiflorus</i>	J	Australia	MN916077	MN904446	MN915578	MN916279	MN915811
<i>Synostemon hirtellus</i>	J	Queensland, Australia	EU623573	GQ503447	GQ503508	EU643763	GQ503574
<i>Synostemon sphenophyllus</i>	J	Queensland, Australia	GQ503402	GQ503465		EU643780	GQ503597
<i>Synostemon trachyspermus</i>	J	Australia	GQ503407	GQ503470	GQ503528	EU643784	GQ503602

Supplementary table S9-2. Matrices with dispersal rate scaling used in reconstruction under the dispersal-extinction-cladogenesis model (DEC). Biogeographic regions follow figure 1: A, North America to Mexico; B, West Indies; C, South America and part of the Panama Isthmus; D, West Africa with eastern border following Namibia, Democratic Republic of Congo and Central African Republic; E, South and Eastern Africa; F, Madagascar and the Mascarene Islands; G, W. Asia stretching from India to Peninsular Malaysia; H, W. Malesia including Philippines; I, E. Malesia (mainly Papua New Guinea); J, Australia; K, Islands in the Pacific. Green marks an increase in dispersal rates, while yellow marks a decrease compared to older periods.

32-60 Ma	A	B	C	D	E	F	G	H	I	J	K
A	1	1	0,5	1	0,01	0,01	1	0,01	0,01	0,01	0,01
B	1	1	0,5	0,5	0,01	0,01	0,01	0,01	0,01	0,01	0,01
C	0,5	0,5	1	0,75	0,25	0,01	0,01	0,01	0,01	0,25	0,01
D	1	0,5	0,75	1	1	0,5	1	0,5	0,01	0,01	0,01
E	0,01	0,01	0,25	1	1	1	0,5	0,5	0,01	0,01	0,01
F	0,01	0,01	0,01	0,5	1	1	0,5	0,5	0,5	0,5	0,01
G	1	0,01	0,01	1	0,5	0,5	1	1	0,01	0,01	0,01
H	0,01	0,01	0,01	0,5	0,5	0,5	1	1	0,5	0,5	0,01
I	0,01	0,01	0,01	0,01	0,01	0,5	0,01	0,5	1	0,75	0,75
J	0,01	0,01	0,25	0,01	0,01	0,5	0,01	0,5	0,75	1	0,75
K	0,01	0,01	0,01	0,01	0,01	0,01	0,01	0,01	0,75	0,75	1

5-32 MA	A	B	C	D	E	F	G	H	I	J	K
A	1	1	1	0,01	0,01	0,01	0,01	0,01	0,01	0,01	0,01
B	1	1	1	0,5	0,01	0,01	0,01	0,01	0,01	0,01	0,01
C	1	1	1	0,5	0,01	0,01	0,01	0,01	0,01	0,01	0,01
D	0,01	0,5	0,5	1	1	0,5	0,75	0,5	0,01	0,01	0,01
E	0,01	0,01	0,01	1	1	1	0,75	0,5	0,01	0,01	0,01
F	0,01	0,01	0,01	0,5	1	1	0,5	0,5	0,5	0,5	0,01
G	0,01	0,01	0,01	0,75	0,75	0,5	1	1	0,5	0,5	0,01
H	0,01	0,01	0,01	0,5	0,5	0,5	1	1	0,5	0,01	0,01
I	0,01	0,01	0,01	0,01	0,01	0,5	0,5	0,5	1	0,75	0,75
J	0,01	0,01	0,01	0,01	0,01	0,5	0,5	0,01	0,75	1	0,75
K	0,01	0,01	0,01	0,01	0,01	0,01	0,01	0,01	0,75	0,75	1

0-5 MA	A	B	C	D	E	F	G	H	I	J	K
A	1	1	1	0,01	0,01	0,01	0,01	0,01	0,01	0,01	0,01
B	1	1	1	0,25	0,01	0,01	0,01	0,01	0,01	0,01	0,01
C	1	1	1	0,25	0,01	0,01	0,01	0,01	0,01	0,01	0,01
D	0,01	0,25	0,25	1	1	0,5	0,5	0,5	0,01	0,01	0,01
E	0,01	0,01	0,01	1	1	1	0,5	0,5	0,01	0,01	0,01
F	0,01	0,01	0,01	0,5	1	1	0,5	0,5	0,5	0,5	0,01
G	0,01	0,01	0,01	0,5	0,5	0,5	1	1	0,75	0,5	0,01
H	0,01	0,01	0,01	0,5	0,5	0,5	1	1	1	0,75	0,25
I	0,01	0,01	0,01	0,01	0,01	0,5	0,75	1	1	1	0,75
J	0,01	0,01	0,01	0,01	0,01	0,5	0,5	0,75	1	1	0,75
K	0,01	0,01	0,01	0,01	0,01	0,01	0,01	0,25	0,75	0,75	1

